TABLE 2. Results of Visual Acuity and FMERG in Preoperative Setting According to IS/OS Status

	IS/OS Status		
	Intact, $n = 7$	Disrupted, $n = 10$	P
Visual acuity, mean ± SE, logMAR (Snellen)	0.3 ± 0.1 (20/44)	0.5 ± 0.1 (20/58)	0.252
Amplitude, mean ± SE, μV			
a-Wave	1.2 ± 0.1	0.9 ± 0.10	0.126
b-Wave	2.6 ± 0.2	1.5 ± 0.2	0.001
OPs	1.1 ± 0.1	0.7 ± 0.1	0.010
Implicit time, mean ± SE, ms			
a-Wave	25 ± 0.5	27 ± 0.7	0.049
b-Wave	46 ± 0.9	50 ± 1.1	0.010

Student's t-test.

than the corresponding layers of the normal fellow eyes ($P < 0.05$, Student's t-test).

After the surgery, the total, inner, and middle retinal layers were significantly thinner at 3 and 6 months than the preoperative thicknesses (Fig. 3 and Table 1; $P < 0.01$, Wilcoxon signed rank test). The reduction occurred mainly during the first 3 months. The thickness of the outer retinal layer did not change until 6 months after the surgery (Fig. 3 and Table 1). There were no significant differences among the thicknesses between the 2 postoperative times.

Focal Macular Electroretinograms

Representative FMERGs from 5 patients recorded before surgery and 6 months postoperatively are shown in Figure 2B. In all cases, the amplitude of the b-waves and OPs increased after surgery, especially in case 5. However, in most cases the FMERGs did not recover to the normal range. The mean amplitudes of the a-waves, b-waves, and sum of OPs and the mean implicit times of the a-waves and b-waves, recorded before surgery and 3 and 6 months postoperatively, are shown in Table 1. The implicit time of b-waves was significantly shorter at 3 and 6 months after the surgery (Wilcoxon singed rank test). The amplitudes of the b-waves and OPs increased significantly at 6 months after surgery (Wilcoxon signed rank test) but that of the a-waves did not change significantly. The mean amplitude of the OPs at 6 months postoperatively was 1.6 times larger than the preoperative amplitude, and the mean amplitude of the b-wave was 1.2 times larger than that of the preoperative b-wave.

Integrity of Photoreceptor IS/OS Junction Line

From the preoperative SD-OCT images, we classified 7 eyes (41%) as having an intact IS/OS line, while 10 eyes (59%) had disrupted IS/OS lines. There were no significant differences in visual acuity and amplitude of the a-wave between the 2 groups (Student's t-test, Table 2). However, there were significant differences in the amplitudes of the b-wave and OPs and the implicit times of the a- and b-waves between the 2 groups (Student's t-test, Table 2).

Correlation Between Retinal Layer Thickness and FMERG Components After ERM Surgery

We determined whether the change of each retinal layer thickness was significantly associated with the improvement of the BCVA and with each component of the FMERGs. We determined the correlation between preoperative and 6 months' postoperative values. An improvement of the BCVA was not correlated with the ratios of the 6 months' postoperative to the preoperative thicknesses at the parafovea for all retinal layers (Supplementary Fig. S1). The 6 M-post/preoperative ratios of the b-wave amplitude were correlated with the post/preoperative ratios of the parafoveal thickness of the total retina ($r = -0.55$, $P = 0.028$, Spearman rank correlation test) and that of the middle retina ($r = -0.51$, $P = 0.042$; Fig. 4). The 6 M-post/preoperative ratios of the sum of the OPs amplitude were also significantly correlated with the post/preoperative ratios of the total retinal thickness ($r = -0.74$,

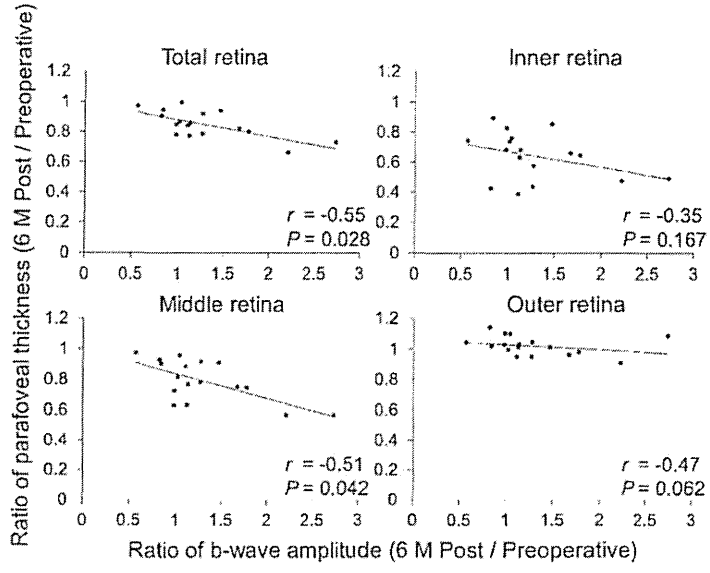

FIGURE 4. Correlations between pre- and postoperative ratios of the b-wave amplitudes at 6 months and the pre- and postoperative ratios of the macular thickness at 6 months. The ratios of the b-wave amplitudes are significantly correlated with the ratios of total and middle retinal thickness (Spearman rank correlation test).

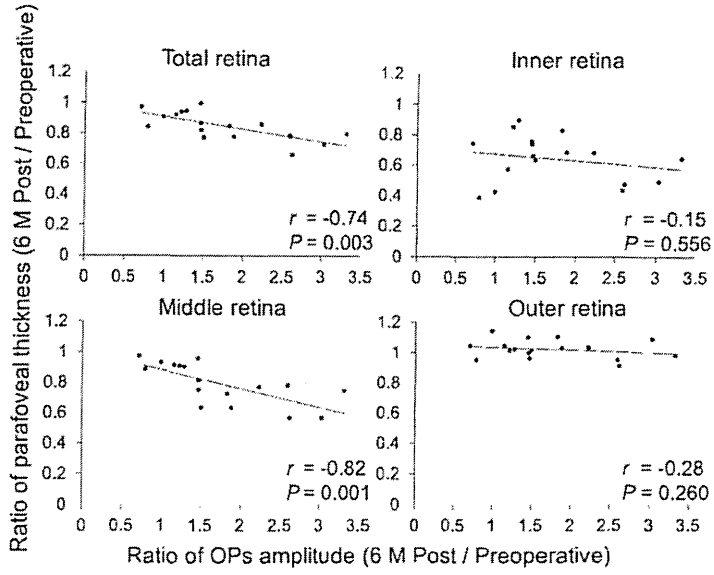

FIGURE 5. Correlations between the pre- and postoperative ratios of the OP amplitude and the pre- and postoperative ratios of the macular thickness at 6 months. The ratios of the OP amplitudes are significantly correlated with the pre- and postoperative ratios of the total and middle retinal thickness (Spearman rank correlation test).

$P = 0.003$) and that of the middle retina ($r = -0.82$, $P = 0.001$; Fig. 5). The coefficient of correlation was higher for the OPs than for the b-waves. In addition, the change of the b-wave implicit time was significantly correlated with the post/preoperative ratios of the middle retinal thickness ($r = 0.50$, $P = 0.046$; Fig. 6).

DISCUSSION

Our SD-OCT results showed that the parafoveal thickness of the inner and middle retinal layers was significantly decreased but the outer retina did not change significantly after the ERM surgery. The mean amplitudes of the FMERG b-waves and OPs were significantly larger postoperatively than those recorded preoperatively. We then determined whether the changes in the thickness of each retinal layer were significantly correlated with the increase in the amplitudes and implicit times of the FMERG. Our analysis showed that the change of thickness in the middle layer, but not inner and outer layer, was significantly correlated with the increase of b-wave and OP amplitude and shortening of b-wave implicit time after ERM peeling. Thus, we confirmed that the improvement of FMERGs by ERM peeling was associated mainly with a reduction of the thickness of the middle retinal layer. Because the coefficient of correlation was

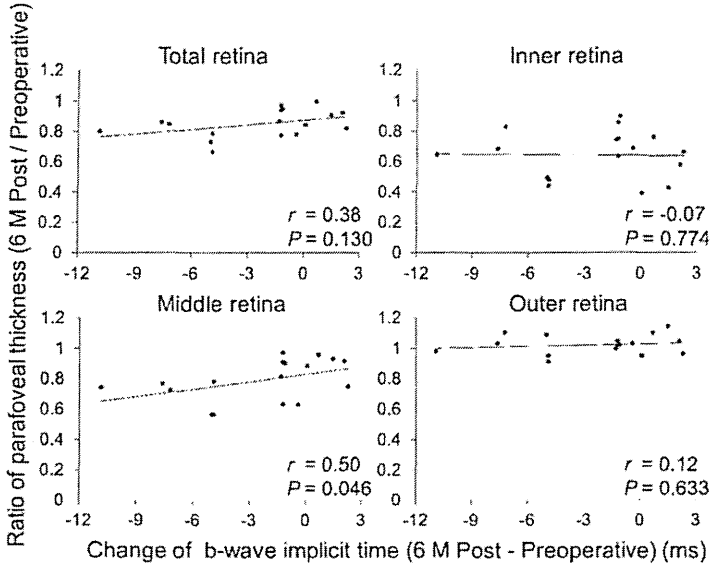

FIGURE 6. Correlations between difference of the b-wave implicit times at 6 months and the pre/postoperative ratios of the macular thickness at 6 months. The difference of the b-wave amplitudes is significantly correlated with the ratios of middle retinal thickness (Spearman rank correlation test).

higher for the relative amplitudes of the OPs than for the b-waves, improvements in the amplitude of the OPs were more strongly correlated with the change in the middle retinal layer thickness than were those of b-waves.

We have reported that the reduction in the amplitude of OPs was significantly greater than that of a-waves and b-waves of the FMERGs of patients with ERM. From these results, we suggest that the ERM probably induces damage mainly to the inner retinal neurons, including the retina from the INL to GCL, because these FMERG components are similarly changed in eyes with cystoid macular edema, which is known to damage the inner retina.[16] We have reported in another study that the reduction of the OPs of the FMERGs does not recover to the normal range after ERM surgery.[17] We assumed that the functional alterations in eyes with an ERM occurs mainly from greater impairment of the inner retina than the outer retina. However, in these studies, we have not been able to confirm the relationship between the thicknesses of the different retinal layers and the FMERG components because of the lower resolution of the OCT instruments at that time. The advancements of OCT technology have enabled us to confirm our earlier assumptions in this study.

A study of the origins of FMERG components, using pharmacologic techniques in monkey retinas, has shown that the b-waves of the FMERGs originate mainly from the ON bipolar cells with additional contribution from the OFF bipolar cell pathway.[32] On the other hand, the origin of the OPs seems to be more from the inner retina than the ON bipolar cells. The results of several full-field ERG studies have suggested that the retinal amacrine cells are the origin of OPs.[33–35] The cell bodies of the ON bipolar cells and amacrine cells are both located in INL, with those of the ON bipolar cells located more in the outer section of the INL and those of the amacrine cells located in the inner section of the INL.[36] We assumed that this difference of location would affect their susceptibility to ERM damage.

One of the commonly used methods to assess macular function is visual acuity. Several studies have examined the relationship between the retinal cell layers and the BCVA in eyes with an ERM.[8,9,12] Kim et al.[9] report that the preoperative parafoveal thicknesses of the GCL+IPL and INL are significantly associated with the preoperative BCVA. Other studies have shown that the degree of metamorphopsia is associated with the macular thickness of the INL.[10–12] These results suggest a similar pathophysiology in eyes with an ERM, indicating that an ERM affects the inner retina more than the outer retina. However, our results showed that the improvement of the BCVA postoperatively was not significantly correlated with the changes in the parafoveal thickness of any of the retinal layers. Even though the BCVA is a relatively easy way to assess the physiology of the fovea, it can be affected by other conditions, such as astigmatism, corneal haze, and cataracts. Because all of our patients underwent cataract surgery, the improvements in the BCVA may have been partially caused by the cataract surgery. This would then mask the relationship with the retinal structure. In addition, the number of patients may have been too low to detect a significant correlation between the thicknesses of the retinal layers and the BCVA.

Other studies have shown that the visual function is significantly associated with the alignment of the photoreceptors.[8,27] Our results also showed that the macular function of eyes that had disrupted IS/OS lines was impaired compared to that of eyes that had intact IS/OS lines. Because the ERMs are located on the surface of the retina, the ERM may disturb the inner retina predominantly in the early stages but the damage may progress to the outer retina in advanced stages.

Our results showed that the amplitudes of the FMERG components were not significantly correlated with the inner retinal thickness. However, this does not mean that the function of the retinal ganglion cells was preserved in eyes with an ERM because the FMERG components analyzed do not originate from the retinal ganglion cell activity.

There were 2 limitations in this study. The first limitation was that we could not measure the macular thickness by macular thickness map owing to the limitation of software. A macular thickness map may allow us to analyze the retinal cell layer 3-dimensionally and to evaluate the retinal structure more precisely. The second limitation was that we did not obtain microperimetry data. It might have helped us to get more information about the sensitivity of each point of retina analyzed by OCT.

In conclusion, the significant correlations between the thickness of the middle retinal layer and the amplitude of the b-waves and OPs suggest that the improvement of macular function after ERM peeling is mainly due to the decrease in the thickness of the middle retinal layer.

Acknowledgments

We thank Duco I. Hamasaki for discussions and editing the manuscript.

Supported by Grant-in-Aid for Scientific Research C (No. 25462709 [SUJ]) from the Ministry of Education, Culture, Sports, Science and Technology (http://www.jsps.go.jp/). The authors alone are responsible for the content and writing of the paper.

Disclosure: **N. Hibi**, None; **S. Ueno**, None; **Y. Ito**, None; **C.-H. Piao**, None; **M. Kondo**, None; **H. Terasaki**, None

References

1. McCarty DJ, Mukesh BN, Chikani V, et al. Prevalence and associations of epiretinal membranes in the visual impairment project. *Am J Ophthalmol.* 2005;140:288–294.
2. Aso H, Iijima H, Imai M, Gotoh T. Temporal changes in retinal thickness after removal of the epiretinal membrane. *Acta Ophthalmol.* 2009;87:419–423.
3. Massin P, Allouch C, Haouchine B, et al. Optical coherence tomography of idiopathic macular epiretinal membranes before and after surgery. *Am J Ophthalmol.* 2000;130:732–739.
4. Treumer F, Wacker N, Junge O, Hedderich J, Roider J, Hillenkamp J. Foveal structure and thickness of retinal layers long-term after surgical peeling of idiopathic epiretinal membrane. *Invest Ophthalmol Vis Sci.* 2011;52:744–750.
5. Kim J, Rhee KM, Woo SJ, Yu YS, Chung H, Park KH. Long-term temporal changes of macular thickness and visual outcome after vitrectomy for idiopathic epiretinal membrane. *Am J Ophthalmol.* 2010;150:701–709.
6. Suh MH, Seo JM, Park KH, Yu HG. Associations between macular findings by optical coherence tomography and visual outcomes after epiretinal membrane removal. *Am J Ophthalmol.* 2009;147:473–480.
7. Wilkins JR, Puliafito CA, Hee MR, et al. Characterization of epiretinal membranes using optical coherence tomography. *Ophthalmology.* 1996;103:2142–2151.
8. Arichika S, Hangai M, Yoshimura N. Correlation between thickening of the inner and outer retina and visual acuity in patients with epiretinal membrane. *Retina.* 2010;30:503–508.
9. Kim JH, Kang SW, Kong MG, Ha HS. Assessment of retinal layers and visual rehabilitation after epiretinal membrane removal. *Graefes Arch Clin Exp Ophthalmol.* 2013;251:1055–1064.
10. Lim JW. Results of spectral-domain optical coherence tomography by preferential hyperacuity perimeter in patients after

idiopathic epiretinal membrane surgery. *Curr Eye Res.* 2011; 36:364-369.

11. Okamoto F, Sugiura Y, Okamoto Y, Hiraoka T, Oshika T. Associations between metamorphopsia and foveal microstructure in patients with epiretinal membrane. *Invest Ophthalmol Vis Sci.* 2012;53:6770-6775.
12. Watanabe A, Arimoto S, Nishi O. Correlation between metamorphopsia and epiretinal membrane optical coherence tomography findings. *Ophthalmology.* 2009;116:1788-1793.
13. Lim JW, Cho JH, Kim HK. Assessment of macular function by multifocal electroretinography following epiretinal membrane surgery with internal limiting membrane peeling. *Clin Ophthalmol.* 2010;4:689-694.
14. Moschos M, Apostolopoulos M, Ladas J, et al. Assessment of macular function by multifocal electroretinogram before and after epimacular membrane surgery. *Retina.* 2001;21:590-595.
15. Lai TY, Kwok AK, Au AW, Lam DS. Assessment of macular function by multifocal electroretinography following epiretinal membrane surgery with indocyanine green-assisted internal limiting membrane peeling. *Graefes Arch Clin Exp Ophthalmol.* 2007;245:148-154.
16. Tanikawa A, Horiguchi M, Kondo M, Suzuki S, Terasaki H, Miyake Y. Abnormal focal macular electroretinograms in eyes with idiopathic epimacular membrane. *Am J Ophthalmol.* 1999;127:559-564.
17. Niwa T, Terasaki H, Kondo M, Piao CH, Suzuki T, Miyake Y. Function and morphology of macula before and after removal of idiopathic epiretinal membrane. *Invest Ophthalmol Vis Sci.* 2003;44:1652-1656.
18. Parisi V, Coppe AM, Gallinaro G, Stirpe M. Assessment of macular function by focal electroretinogram and pattern electroretinogram before and after epimacular membrane surgery. *Retina.* 2007;27:312-320.
19. Suzuki T, Terasaki H, Niwa T, Mori M, Kondo M, Miyake Y. Optical coherence tomography and focal macular electroretinogram in eyes with epiretinal membrane and macular pseudohole. *Am J Ophthalmol.* 2003;136:62-67.
20. Terasaki H, Kojima T, Niwa H, et al. Changes in focal macular electroretinograms and foveal thickness after vitrectomy for diabetic macular edema. *Invest Ophthalmol Vis Sci.* 2003;44: 4465-4472.
21. Terasaki H, Ishikawa K, Niwa Y, et al. Changes in focal macular ERGs after macular translocation surgery with 360 degrees retinotomy. *Invest Ophthalmol Vis Sci.* 2004;45:567-573.
22. Sugita T, Kondo M, Piao CH, Ito Y, Terasaki H. Correlation between macular volume and focal macular electroretinogram in patients with retinitis pigmentosa. *Invest Ophthalmol Vis Sci.* 2008;49:3551-3558.
23. Nishihara H, Kondo M, Ishikawa K, et al. Focal macular electroretinograms in eyes with wet-type age-related macular degeneration. *Invest Ophthalmol Vis Sci.* 2008;49:3121-3125.
24. Ishikawa K, Nishihara H, Ozawa S, et al. Focal macular electroretinograms after photodynamic therapy combined with intravitreal bevacizumab. *Graefes Arch Clin Exp Ophthalmol.* 2011;249:273-280.
25. Iwata E, Ueno S, Ishikawa K, et al. Focal macular electroretinograms after intravitreal injections of bevacizumab for age-related macular degeneration. *Invest Ophthalmol Vis Sci.* 2012;53:4185-4190.
26. Srinivasan VJ, Wojtkowski M, Witkin AJ, et al. High-definition and 3-dimensional imaging of macular pathologies with high-speed ultrahigh-resolution optical coherence tomography. *Ophthalmology.* 2006;113:2054-2065.
27. Inoue M, Morita S, Watanabe Y, et al. Inner segment/outer segment junction assessed by spectral-domain optical coherence tomography in patients with idiopathic epiretinal membrane. *Am J Ophthalmol.* 2010;150:834-839.
28. Wojtkowski M, Bajraszewski T, Gorczynska I, et al. Ophthalmic imaging by spectral optical coherence tomography. *Am J Ophthalmol.* 2004;138:412-419.
29. Miyake Y, Shiroyama N, Ota I, Horiguchi M. Oscillatory potentials in electroretinograms of the human macular region. *Invest Ophthalmol Vis Sci.* 1988;29:1631-1635.
30. Miyake Y. Studies of local macular ERG [in Japanese]. *Nippon Ganka Gakkai Zasshi.* 1988;92:1419-1449.
31. Sakai T, Kondo M, Ueno S, Koyasu T, Komeima K, Terasaki H. Supernormal ERG oscillatory potentials in transgenic rabbit with rhodopsin P347L mutation and retinal degeneration. *Invest Ophthalmol Vis Sci.* 2009;50:4402-4409.
32. Kondo M, Ueno S, Piao CH, Miyake Y, Terasaki H. Comparison of focal macular cone ERGs in complete-type congenital stationary night blindness and APB-treated monkeys. *Vision Res.* 2008;48:273-280.
33. Korol S, Leuenberger PM, Englert U, Babel J. In vivo effects of glycine on retinal ultrastructure and averaged electroretinogram. *Brain Res.* 1975;97:235-251.
34. Nakatsuka K, Hamasaki DI. Destruction of the indoleamine-accumulating amacrine cells alters the ERG of rabbits. *Invest Ophthalmol Vis Sci.* 1985;26:1109-1116.
35. Wachtmeister L. Oscillatory potentials in the retina: what do they reveal. *Prog Retin Eye Res.* 1998;17:485-521.
36. Kolb H, Famiglietti EV. Rod and cone pathways in the inner plexiform layer of cat retina. *Science.* 1974;186:47-49.

Int Ophthalmol
DOI 10.1007/s10792-013-9855-y

ORIGINAL PAPER

Transient increase of retinal nerve fiber layer thickness after macular hole surgery

Nobuaki Hibi · Mineo Kondo · Kohei Ishikawa · Shinji Ueno · Keiichi Komeima · Hiroko Terasaki

Received: 27 March 2013 / Accepted: 14 September 2013

Abstract We studied the changes in the thickness of the retinal nerve fiber layer (RNFL) after surgery for idiopathic macular hole (MH) using spectral-domain optical coherence tomography (SD-OCT). Twenty eyes of 20 consecutive patients who underwent vitrectomy to close a MH were studied. The peripapillary RNFL thickness was measured by SD-OCT before and at 1, 3, and 6 months after surgery. The mean overall thickness, the thickness of the four quadrants, and the thickness of each of the 12 clock hours of the RNFL were analyzed. The mean overall RNFL thickness before surgery was 93.3 ± 9.6 μm, and it increased significantly to 98.7 ± 7.4 μm at 1 month after surgery ($P < 0.05$). The mean overall thickness then returned to the pre-surgery level at three and 6 months. The transient increase of RNFL thickness at 1 month after surgery was statistically significant in the superior, nasal, and inferior quadrants. The increase in the thickness of the nasal quadrants was maintained for up to 6 months. When the thickness of the individual 12 clock hours were analyzed, the transient increase of RNFL thickness at 1 month after surgery was significant at each of the 0–5 o'clock positions. The transient increase in the RNFL thickness after MH surgery may be caused by mild edema of the inner retinal layers caused by the MH surgery.

Keywords Macular hole · Retinal nerve fiber layer · Surgery · Optical coherent tomography

N. Hibi · K. Ishikawa · S. Ueno · K. Komeima · H. Terasaki
Department of Ophthalmology, Nagoya University Graduate School of Medicine, Nagoya, Japan

M. Kondo (✉)
Department of Ophthalmology, Mie University Graduate School of Medicine, 2-174 Edobashi, Tsu 514-8507, Japan
e-mail: mineo@clin.medic.mie-u.ac.jp

Published online: 28 September 2013

Background

The rate of an anatomical closure of an idiopathic macular hole (MH) by vitrectomy with internal limiting membrane (ILM) peeling is very high, and the closure is accompanied by significant visual improvements in most cases [1–4]. Although MH surgery has generally been considered to be a safe procedure, various complications have been reported. One of the most serious complications is the development of visual field defects in the peripheral retina [5–10]. The exact mechanism causing the visual field defects after the surgery has still not been definitively determined, but it has been postulated that the defects are caused by inner retinal damage due to air-flow drying during the infusion of air through the canula [11, 12], prolonged gas tamponade [6, 7], or the removal of the posterior hyaloid membrane [6, 7, 9].

We have previously recorded full-field electroretinograms before and after MH surgery [13], and found that the amplitude of the photopic negative

response (PhNR) was significantly reduced after MH surgery even though the patients did not have any visual field defects. However, the amplitude of the photopic a- and b-waves was not significantly altered. Because the PhNR is believed to originate mainly from the electrical activity of ganglion cells and their axons, these results suggested that there may be functional impairments of the inner retina after MH surgery.

These results motivated us to examine the morphological changes of the inner retinal layers before and after MH surgery. Several studies have been published on the morphological changes of the inner retinal layer after MH surgery using scanning laser polarimeter [14] and optical coherence tomography (OCT) [15–18], but the results were very different among these reports.

Thus, the purpose of this study was to investigate the changes in the retinal nerve fiber layer (RNFL) thickness before and after surgery for idiopathic MH. To accomplish this, we examined the retinas by spectral-domain OCT (SD-OCT) before and after MH surgery. We shall show that the mean RNFL thickness increased 1 month after surgery, but then returned to the pre-surgical level at 3 and 6 months after surgery. The possible causes of this transient increase of the RNFL thickness are discussed.

Methods

Subjects

We prospectively studied 20 eyes of 20 consecutive patients (11 male, 9 female) who were scheduled to undergo vitrectomy for an idiopathic MH at the Nagoya University Hospital from March 2009 to September 2010. This study was approved by the Institutional Review Board of the Nagoya University Graduate School of Medicine. All examinations and investigations adhered to the tenets of the Declaration of Helsinki. Informed consent was obtained from each of the patients after an explanation of the procedures to be used and possible complications.

The age of the patients ranged from 44–76 years (mean 63.3 ± 8.4). Patients who were taking glaucoma medications or had visual field defects were excluded. The MH of 10 eyes were at stage 2, eight eyes at stage 3, and two eyes at stage 4 according to the Gass classification [19, 20].

Surgical procedures

Standard three-port pars plana vitrectomy was performed on all eyes either with a 20 gauge system (17 eyes) or 23 gauge system (3 eyes). After a core vitrectomy, triamcinolone acetonide (Kenakolt; Bristol-Myers-Squibb, New York, USA) was injected into the vitreous cavity to make the vitreous gel more visible. A posterior vitreous detachment (PVD) was then created by suction with the vitreous cutter unless a PVD was already present. As much of the vitreous was removed as possible.

The ILM was then grasped with forceps, peeled, and removed. After fluid–air exchange by passive aspiration with a backflush needle, 0.6 ml of 100 % sulfur hexafluoride (SF6) gas was injected into the vitreous cavity. Postoperatively, all patients were asked to maintain a face-down position for about 7 days.

Peripapillary RNFL thickness

SD-OCT was performed with the Cirrus HD-OCT (software version 3.0) (Carl Zeiss Meditec Inc.) before and at 1, 3, and 6 months after MH surgery. The principles of SD-OCT have been described in detail [21]. The scan speed for Cirrus is 27,000 A-scans/sec and the axial resolution is 5 μm. The fast RNFL scan protocol (software version 3.0) was used to measure the peripapillary RNFL thickness. The scan consisted of 256 radial axial scans along a circle with a diameter of 3.46 mm. The center of the scan was manually positioned at the center of the optic disc.

Three types of analysis of the RNFL thickness were made. The first was the average of the RNFL thickness over the entire circumference (256 values) of the optic disc, i.e., the average overall RNFL thickness. The second was the thickness of the RNFL in the four quadrants—superior (46–135°), nasal (136–225°), inferior (226–315°), and temporal (316–45°) quadrants. The third was the RNFL thickness at each of the 12 clock hours. The right eye orientation was used for the clock hour designations. All of the OCT scans had a signal strength ≥7.

Visual acuity and visual fields

The visual acuity was measured before, and at 1, 3, and 6 months after surgery with a standard Japanese visual acuity chart, and the decimal visual acuity was

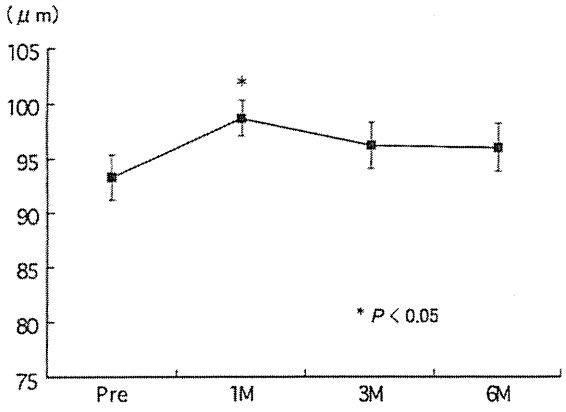

Fig. 1 Changes in the average overall RNFL thickness before and at 1, 3, and 6 months after MH surgery. *Bars* indicate the standard error of the means of 20 eyes; $*P < 0.05$

converted to the logarithm of the minimum angle of resolution (logMAR) units for statistical analyses. We also performed Goldmann perimetry before and at 6 months after surgery (stimulus sizes I2, I3, I4, and V4).

Statistical analyses

The significance of the differences in best-corrected visual acuity (BCVA) and RNFL thickness between pre-operative and post-operative values was determined by the Wilcoxon signed rank test. Differences were considered to be significant when the P value was <0.05.

Results

The MH was closed in all 20 eyes after a single surgery. The BCVA was 0.74 ± 0.24 (mean ± SD) before surgery, and it significantly improved to 0.49 ± 0.19, 0.36 ± 0.23, and 0.30 ± 0.20 at 1, 3, and 6 months after surgery, respectively ($P < 0.05$). None of the eyes had any visual field defects when examined by Goldmann perimetry at 6 months after surgery. In addition, none of the patients had any visual complaints after surgery.

Peripapillary RNFL thickness

The average overall RNFL thickness was 93.3 ± 9.6 μm before surgery, and the thickness increased significantly to 98.7 ± 7.4 μm (5.5 % increase) 1 month after surgery ($P < 0.05$, Fig. 1). The overall thickness then decreased to 96.2 ± 9.7 μm at three and 96.0 ± 10.0 μm at 6 months after surgery. The RNFL thickness at 3 and 6 months after surgery was not significantly different from the preoperative value.

The RNFL thickness in each of the four quadrants was significantly increased at 1 month but then returned to the pre-surgery level at 6 months after surgery in the superior and inferior quadrants (Fig. 2). The RNFL thickness in the nasal quadrant was significantly thicker at 1 month after surgery and remained thicker at 6 months after the surgery. In the temporal quadrant, the RNFL was thicker at 1 month but this increase was not statistically significant. Figure 3 shows representative color maps of the overall and four quadrant RNFL thicknesses before and after surgery for a 60-year-old woman. An increase in the RNFL thickness after surgery can be seen in the nasal, superior and inferior quadrants.

To examine the changes in the RNFL thickness more finely, we analyzed the changes in the RNFL thickness before and after surgery at each of the 12 clock hours (Table 1). At each clock hour between 6 and 11 clock hours, there was no significant difference in the RNFL thickness before and after surgery. On the other hand, the RNFL thickness increased significantly at 1 month after surgery between the 0 and 5 clock hours. At 3 months after surgery, there were five regions (0, 1, 3, 4, and 5 clock hours) where the RNFL was significantly thicker than before surgery. At 6 months after surgery, there were still four regions (0, 1, 3, and 4 clock hours) where the RNFL was significantly thicker than before surgery.

The relative RNFL thicknesses after surgery compared to before surgery are shown in Fig. 4. We found that at 1 month after surgery, the mean relative RNFL thickness increased >10 % at four regions—0, 1, 3, and 4 clock hours. At 3 and 6 months, there were still two regions, 3 and 4 clock hours, where the mean relative RNFL was still thicker by 10 % than before surgery.

Discussion

There are several studies on the morphological changes of the inner retinal layer after MH surgery [14–18]. Ebisawa et al. [14] used scanning laser polarimetry to

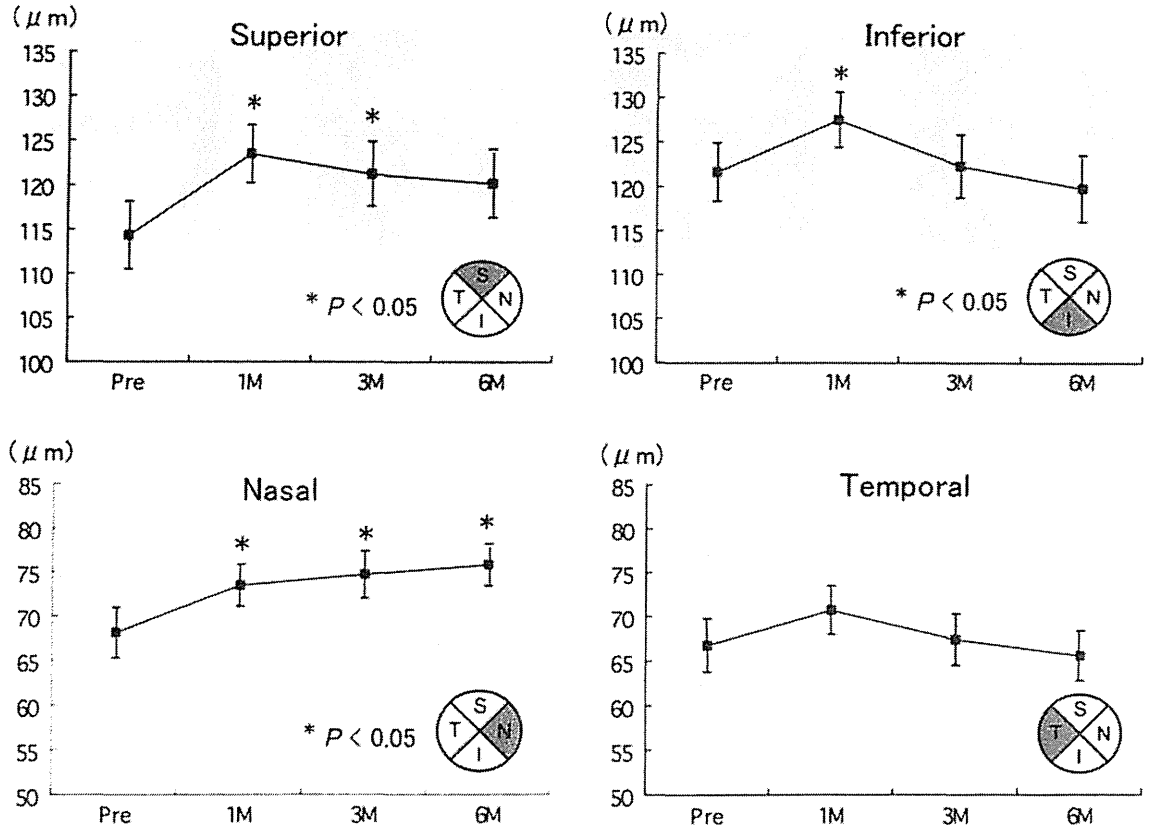

Fig. 2 Changes in the average RNFL thickness in the four quadrants before and at 1, 3, and 6 months after MH surgery. *Bars* indicate the standard error of the means of 20 eyes; $*P < 0.05$

study the changes in the RNFL thickness before and after MH surgery without ILM peeling. They reported that the RNFL thickness decreased significantly up to 3 months after MH surgery, but it then increased up to 12 months to the preoperative thickness. They found that the decrease of RNFL thickness was more severe in cases with visual field defects after surgery, and concluded that the visual field defects were due to inner retinal damage caused by the surgery. In 2006, Yamashita et al. [15] studied the RNFL thickness after MH surgery with ILM peeling using time-domain OCT, and reported that the decrease of RNFL thickness after surgery was more severe in eyes with visual field defects than in eyes without visual field defects. Brazititos et al. [16] also measured the RNFL thickness by time-domain OCT before and at 6 months after Trypan blue-assisted MH surgery with ILM peeling and did not find any significant changes in the overall peripapillary RNFL thickness or in the four quadrants.

The pattern of the changes in the RNFL thickness after MH surgery in our patients was different from these past reports; in our patients, the overall peripapillary RNFL increased significantly 1 month after surgery and then returned to the pre-surgery level 3 months after surgery. A more detailed regional analysis demonstrated that this transient increase of RNFL was significant in the superior, nasal and inferior quadrants especially at the 0–5 clock hours.

Our findings are very similar to those of Tsuiki et al. [17, 18] who investigated the RNFL thickness before and after vitrectomy with ILM peeling in patients with MH using time-domain OCT. They reported that the RNFL thickness increased at about 1 week after surgery, then returned to pre-surgery level. Although the degree of increase in RNFL thickness after surgery was greater in the study by Tsuiki et al. (10.8–12.5 % at average 8.6 days) than in our study (5.5 % at 1 month), the time-course of the changes of the RNFL

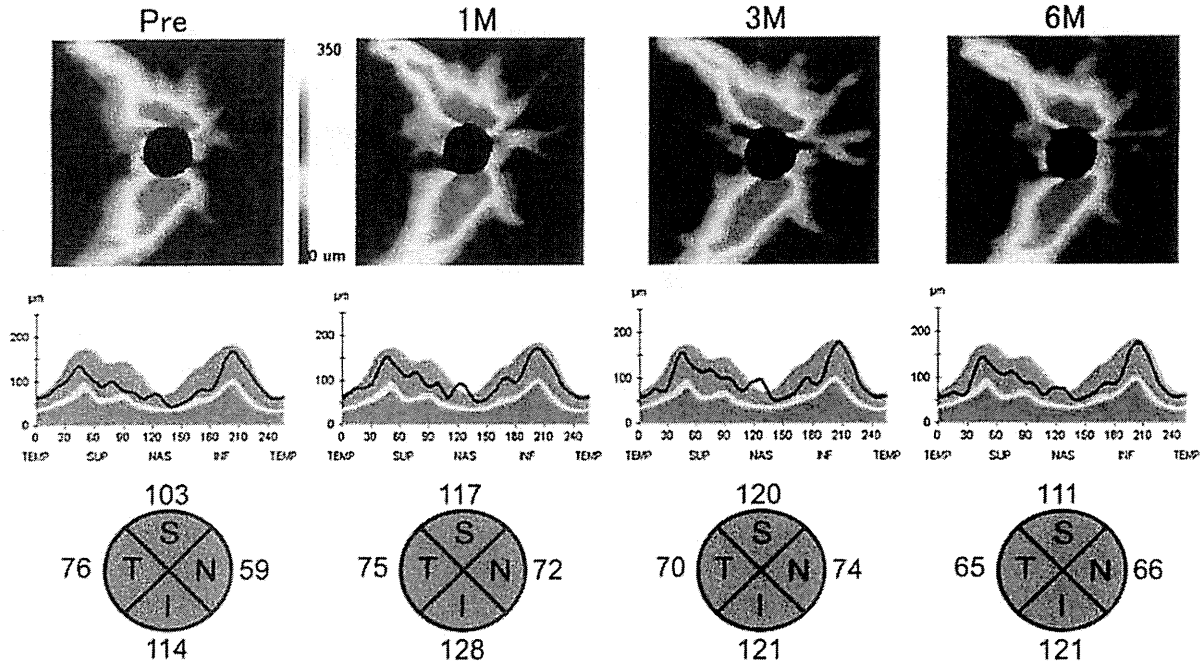

Fig. 3 Color coded maps of the retinal nerve fiber layer (RNFL) thickness (*top panel*), the RNFL thicknesses around the optic disc (*middle panel*), and average RNFL thickness values for the four quadrants of a representative eye before and at 1, 3, and 6 months after surgery. In the RNFL thickness map, false color coding of RNFL thickness with a *scale bar* is displayed. The RNFL thickness increased at the nasal, superior, and inferior quadrants after surgery

Table 1 Changes in the RNFL thickness before and after surgery at 12 clock hour regions

	Pre	1 month	3 months	6 months
0 (superior)	117.2 ± 28.6	129.8 ± 25.2*	128.5 ± 28.1*	125.2 ± 31.0*
1	103.0 ± 21.8	114.0 ± 22.0*	109.6 ± 22.3*	111.1 ± 22.6*
2	81.3 ± 20.0	86.3 ± 18.5*	83.7 ± 13.5	84.8 ± 13.1
3 (nasal)	59.4 ± 12.8	65.6 ± 11.3*	69.1 ± 15.6*	69.5 ± 12.8*
4	61.5 ± 15.4	70.0 ± 12.3*	70.7 ± 15.3*	70.6 ± 14.7*
5	92.7 ± 19.3	99.8 ± 20.5*	97.4 ± 21.3*	96.4 ± 22.2
6 (inferior)	133.7 ± 21.0	138.7 ± 20.3	134.4 ± 22.6	136.5 ± 19.7
7	131.7 ± 34.1	136.7 ± 34.9	131.3 ± 37.7	127.0 ± 37.8
8	70.6 ± 17.4	71.4 ± 14.0	69.0 ± 14.9	67.2 ± 16.9
9 (temporal)	58.4 ± 15.3	58.8 ± 10.1	55.5 ± 11.1	54.2 ± 10.5
10	77.5 ± 19.5	78.7 ± 14.3	75.1 ± 17.8	71.6 ± 16.0
12	119.4 ± 23.1	125.9 ± 21.7	123.1 ± 24.9	120.5 ± 20.8

Right eye orientation was used for documentation of clock hour measurements

* $P < 0.05$

thickness after surgery was very similar to our results. They hypothesized that the transient increase in RNFL thickness after surgery was due to mild edema of the RNFL which was caused by the vitrectomy.

We do not know exactly what procedure of the vitrectomy caused this transient increase in RNFL thickness after MH surgery. There are many papers suggesting that indocyanine green (ICG), which was used to make the ILM more visible, has a toxic effect on the inner retina [22–26]. However, we did not use ICG to stain the ILM during the surgery. If the removal of ILM caused the transient edema of RNFL, the increase of the RNFL thickness should be most prominent in the temporal quadrant. However, our results showed that the transient increase of RNFL was not significant in the temporal quadrant (Fig. 2).

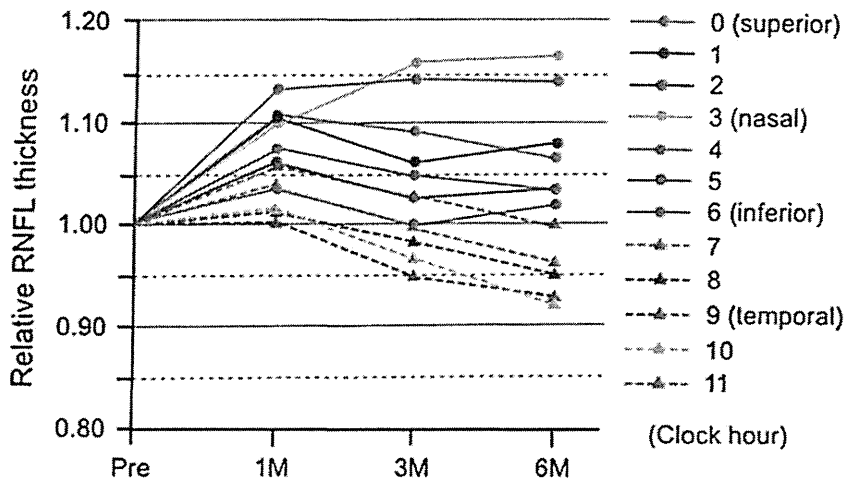

Fig. 4 Changes in the RNFL thickness before and after surgery at each of the 12 clock hours. The RNFL thicknesses are expressed relative to that before surgery. Right eye orientation was used to designate the clock hours

We suggest that the transient increase in the RNFL thickness after vitrectomy results from inner retinal damage induced during the infusion of saline and/or air that are directed against the retinal surface from the cannula during the vitrectomy. Our study showed that the transient increase in RNFL thickness was statistically significant at nasal, upper and lower regions, especially the 0–5 clock hour regions, where the saline and/or air was directed from the infusion cannula. We also believe that saline-induced stress, as well as air, is involved in the transient increase in RNFL thickness because Tsuiki et al. [18] reported that epiretinal membrane removal vitrectomy without air–fluid exchange also causes a transient increase of RNFL thickness.

The time course of the changes in the RNFL thickness after MH surgery depended on the retinal regions. At the 3 and 4 clock hours, the RNFL remained thicker than the pre-treatment level up to 6 months, but at other regions, the RNFL thickness returned to the pre-surgery level or decreased to be thinner than that of the pre-surgery level (Fig. 4). We do not know the exact cause of this different pattern of RNFL thickness at different retinal regions, but this may be due to different degrees of inner retinal damage in the different retinal regions. Long-term follow-up of RNFL thickness after MH surgery or animal experiments may be useful to clarify this question.

We cannot explain why the temporal quadrant of the RNFL thickness did not show the transient increase (Fig. 2). However, the ILM peeling was performed in this area of the nerve fiber layer that feeds this quadrant, and the damage due to the ILM peeling may not be so severe as to cause the transient edema of the RNFL. Another possibility might be that the RNFL damage due to ILM peeling might cause a gradual decrease of the RNFL thickness at a relatively later period after the surgery without any early RNFL increase as seen in Fig. 3.

There are two limitations in this study. The first limitation was that we analyzed the RNFL thickness only in a circle around the optic disc with a diameter of 3.46 mm, and did not measure the RNFL in more peripheral retinal areas. Recent advances in the mapping of the RNFL thickness or ganglion cell complex analysis may provide more useful information. The second limitation was the short follow-up period. We followed the RNFL thickness for 6 months, but the RNFL thickness was still not stabilized at this time. It would be interesting to see how the RNFL thickness at each region changes and stabilizes during the one and 2 years after surgery.

Conclusions

Our results showed that there was a transient increase in the peripapillary RNFL thickness after MH surgery. The increase in the RNFL thickness in the early stages after surgery is probably caused by a slight edema of inner retinal layer caused by the MH surgery.

Acknowledgments The authors thank Duco I. Hamasaki for editing the manuscript. Grant-in-Aid for Scientific Research B (#203904480 HT), and C (#20592075 MK) from Ministry of Education, Culture, Sports, Science and Technology (http://www.jsps.go.jp/).

Conflict of interest The authors declare that they have no conflict of interests.

References

1. Kelly NE, Wendel RT (1991) Vitreous surgery for idiopathic macular holes. Results of a pilot study. Arch Ophthalmol 109:654–659
2. Yooh HS, Brooks HL Jr, Capone A Jr et al (1996) Ultrastructural features of tissue removed during idiopathic macular hole surgery. Am J Ophthalmol 122:67–75
3. Park DW, Sipperley JO, Sneed SR et al (1999) Macular hole surgery with internal-limiting membrane peeling and intravitreous air. Ophthalmology 106:1392–1397
4. Gaudric A (2009) Macular hole sugery. Simple or complex? Am J Ophthalmol 147:381–383
5. Melberg NS, Thomas MA (1995) Visual field loss after pars plana vitrectomy with air/fluid exchange. Am J Ophthalmol 120:386–388
6. Hutton WL, Fuller DG, Snyder WB et al (1996) Visual field defects after macular hole surgery: a new finding. Ophthalmology 103:2152–2158
7. Boldt HC, Munden PM, Folk JC, Mehaffey MG (1996) Visual field defects after macular hole surgery. Am J Ophthalmol 122:371–381
8. Bopp S, Lucke K, Hille U (1997) Peripheral visual field loss after vitreous surgery for macular holes. Graefes Arch Clin Exp Ophthalmol 235:362–371
9. Ezra E, Arden GB, Riordan-Eva P et al (1996) Visual field loss following vitrectomy for stage 2 and 3 macular holes. Br J Ophthalmol 80:519–525
10. Pendergast SD, McCuen BW 2nd (1996) Visual field loss after macular hole surgery. Ophthalmology 103:1069–1077
11. Welch JC (1997) Dehydration injury as a possible cause of visual field defect after pars plana vitrectomy for macular hole. Am J Ophthalmol 124:698–699
12. Hirata A, Yonemura N, Hasumura T et al (2000) Effect of infusion air pressure on visual field defects after macular hole surgery. Am J Ophthalmol 130:611–616
13. Ueno S, Kondo M, Piao CH et al (2006) Selective amplitude reduction of the PhNR after macular hole surgery: ganglion cell damage related to ICG-assisted ILM peeling and gas tamponade. Invest Ophthalmol Vis Sci 47:3545–3549
14. Ebisawa N, Mori K, Yoneya S (2000) Thickness of retinal nerve fiber layer decreases after vitreous surgery for idiopathic macular hole. Nihon Ganka Gakkai Zasshi (Japanese) 104:142–147
15. Yamashita T, Uemura A, Kita H, Sakamoto T (2006) Analysis of the retinal nerve fiber layer after indocyanine green-assisted vitrectomy for idiopathic macular holes. Ophthalmology 113:280–284
16. Brazitikos PD, Katsimpris JM, Tsironi E, Androudi S (2010) Retinal nerve fiber layer thickness evaluation after trypan blue-assisted macular surgery. Retina 30:640–647
17. Tsuiki E, Koga M, kitaoka T (2007) Changes in retinal nerve fiber layer thickness following vitreous surgery. Rinsho Ganka (Japanese) 61:357–360
18. Tsuiki E, Kusano M, Kishikawa Y, Kitaoka T (2008) Changes in the thickness of retinal nerve fiber layer after vitreous surgery for macular hole or epiretinal membrane. Rinsho Ganka (Japanese) 61:347–350
19. Gass JD (1988) Idiopathic senile macular hole: its early stages and pathogenesis. Arch Ophthalmol 106:629–639
20. Gass JD (1995) Reappraisal of biomicroscopic classification of stages of development of a macular hole. Am J Ophthalmol 119:752–759
21. Nassif N, Cense B, Park BH et al (2004) In vivo human retinal imaging by ultrahigh-speed spectral-domain optical coherence tomography. Opt Lett 29:480–482
22. Gandorfer A, Haritoglou C, Gass CA et al (2001) Indocyanine green-assisted peeling of the internal limiting membrane may cause retinal damage. Am J Ophthalmol 132:431–433
23. Gandorfer A, Haritoglou C, Gandorfer A, Kampik A (2003) Retinal damage from indocyanine green in experimental macular surgery. Invest Ophthalmol Vis Sci 44:316–323
24. Haritoglou C, Gandorfer A, Gass CA et al (2002) Indocyanine green-assisted peeling of the internal limiting membrane in macular hole surgery affects visual outcome: a clinicopathologic correlation. Am J Ophthalmol 134:836–841
25. Horio N, Horiguchi M (2004) Effect on visual outcome after macular hole surgery when staining the internal limiting membrane with indocyanine green dye. Arch Ophthalmol 122:992–996
26. Ando F, Yasui O, Hirose H, Ohba N (2004) Optic nerve atrophy after vitrectomy with indocyanine green-assisted internal limiting membrane peeling in diffuse diabetic macular edema: adverse effect of ICG-assisted ILM peeling. Graefes Arch Clin Exp Ophthalmol 242:995–999

Vision Research 91 (2013) 118–123

Contents lists available at ScienceDirect

Vision Research

journal homepage: www.elsevier.com/locate/visres

Focal cone ERGs of rhodopsin Pro347Leu transgenic rabbits

Shinji Ueno [a,*], Toshiyuki Koyasu [a], Taro Kominami [a], Takao Sakai [a], Mineo Kondo [b], Shunsuke Yasuda [a], Hiroko Terasaki [a]

[a] Department of Ophthalmology, Nagoya University Graduate School of Medicine, Nagoya, Japan
[b] Department of Ophthalmology, Mie University Graduate School of Medicine, Tsu, Japan

ARTICLE INFO

Article history:
Received 21 May 2013
Received in revised form 9 August 2013
Available online 21 August 2013

Keywords:
Focal ERG
Retinal degeneration
Transgenic rabbit
Retinitis pigmentosa
Oscillatory potentials
Inner retina

ABSTRACT

A rhodopsin P347L transgenic (Tg) rabbit, a model of retinitis pigmentosa, has been generated in our laboratory. The purpose of this study was to determine the properties of focal areas of the retina in this rabbit model during the course of retinal degeneration. To accomplish this, we recorded focal ERGs from wild-type (WT) and Tg rabbits at ages 3, 6, and 12 months. A 15° stimulus spot was used to elicit the focal ERGs from the center of the visual streak and from four surrounding areas. We found that the amplitudes of the focal cone ERG b-waves and oscillatory potentials (OPs) of the Tg rabbits in the five areas decreased progressively with increasing age and became almost non-recordable at 12 months. There were no significant regional differences in the b-waves of Tg rabbits recorded from the 5 areas. The amplitudes of the OPs were better preserved than the b-waves and the OPs/b-wave ratio was higher than that in WT rabbits at every recording area. The summed OPs amplitudes, which most likely originate from the amacrine and/or ganglion cells, recorded from the area superior to the optic disc was significantly larger than that from other areas at 3- and 6-months-old. This indicated that the inner retinal neurons were not altered equally after photoreceptor degeneration in this rabbit model.

1. Introduction

Retinitis pigmentosa (RP) is a group of inherited retinal diseases caused by mutations of genes related to the retina. These mutations result in degeneration of the rod photoreceptors followed by a gradual loss of cones. Photoreceptor degeneration is followed by the death of the inner retinal cells (Heckenlively, 1988; Weleber, Gregory-Evance, et al., 2006). The retinal degeneration usually begins in the periphery, and the function and morphology of cone-rich central area are relatively well preserved until the late stages of the disease process.

Different subjective and objective examinations have been used to assess the macular function in patients with RP. Among the objective methods, focal ERGs (Ikenoya et al., 2007; Sugita et al., 2008) and multifocal ERGs (Chan & Brown, 1998; Hood et al., 1998; Seeliger et al., 1998; Vajaranant et al., 2002) have been used. Our laboratory has developed a technique for recording focal cone ERGs while monitoring the location of the stimulus on the fundus with an infrared camera during the recordings (Kondo et al., 2008; Miyake, 1990; Miyake et al., 1989; Shiroyama & Miyake, 1990). In our system, focal ERGs can be recorded even in patients without good fixation, and the a- and b-waves and oscillatory potentials (OPs) elicited by focal stimuli resemble full-field cone ERGs.

To study the pathophysiology of RP, we have generated a rhodopsin P347L transgenic (Tg) rabbit using bacterial transgenes (Kondo et al., 2009). We found that the rod function of Tg rabbits was reduced at an early age whereas the cone function was relatively well preserved. We also noted that the oscillatory potentials (OPs), which are believed to originate mainly from amacrine and ganglion cells (Dong, Agey, & Hare, 2004; Wachtmeister, 1998), were larger than those of wild type rabbits (Sakai et al., 2009). Although the exact mechanism(s) underlying these secondary changes in the postreceptoral neurons has not been fully determined, our results indicated that the activities of the inner retinal neurons were altered in Tg rabbits (Marc et al., 2007).

The visual streak of the rabbit retina is a horizontal band lying inferior to the optic nerve head where the densities of rods and cones are higher than elsewhere in the retina (Famiglietti & Sharpe, 1995; Juliusson et al., 1994) Our histopathological study of Tg rabbits showed that the retinal degeneration developed earlier in the visual streak than in other areas (Kondo et al., 2009).

The conclusions made from these earlier ERG studies were mainly based on the results obtained from full-field ERGs, and we do not know whether there are local functional changes in the retina in this rabbit model. Thus, the purpose of this study was to determine the characteristics of local areas of the retina of Tg rabbits by recording focal ERGs. To accomplish this, we

* Corresponding author. Address: 65 Tsuruma-cho, Showa-ku, Nagoya 466-8550, Japan. Fax: +81 52 744 2278.
E-mail address: ueno@med.nagoya-u.ac.jp (S. Ueno).

0042-6989/$ - see front matter © 2013 Elsevier B.V. All rights reserved.
http://dx.doi.org/10.1016/j.visres.2013.08.006

recorded and analyzed the changes in the b-waves and the OPs from 5 regions of the retina of Tg rabbits at 3, 6, and 12 months.

2. Materials and methods

2.1. Animals

The experiments were performed on 8 Tg and 9 wild type (WT) pigmented rabbits whose ages ranged from 3 to 12 months. After recording the ERGs, 1 Tg rabbit was euthanized at 3 months, and 3 WT and 3 Tg rabbits were euthanized at 6 months. All protocols were approved by the Institutional Review Board of Nagoya University Graduate School of Medicine and adhered to the EU Directive 2010/63/EU for animal experiments.

The techniques used for generating the Tg rabbits has been described in detail (Kondo et al., 2009). We used pigmented rabbits, a cross of Dutch pigmented rabbits and New Zealand albino rabbits because the stray light effects are lower in pigmented eyes. The animals were anesthetized with an intramuscular injection of 25 mg/kg ketamine and 2 mg/kg xylazine to record the ERGs.

2.2. Stimuli for focal ERGs

The system for recording focal ERGs consisted of a modified infrared fundus camera and an electronic pulse generator that controlled the light-emitting diodes (LEDs) used for the stimulus and background illumination (Kowa, Nagoya, Japan). An infrared television fundus camera was modified so that the stimuli were presented in Maxwellian view. The images from this fundus camera were fed to a television monitor with a 45° view of the posterior pole of the eye. The position of the stimulus spot on the fundus was monitored on the television screen and could be moved by the examiner with a joystick. A white LED was used for the stimulus and background illumination that covered a retinal area of 45°. The size of the stimulus spot was 15°, and the luminance of the background was fixed at 3 phot cd/m^2 for photopic conditions. The luminance of the stimulus spot was 30 phot cd/m^2, and the stimulus duration was 100 ms for photopic conditions. The luminance of the stimulus spot was 3 phot cd/m^2 and the stimulus duration was 10 ms for scotopic conditions. The stimulus repetition rate was fixed at 2 Hz. The luminance of the stimulus and background illumination was measured at the corneal surface and then converted to the value at the retinal surface. These luminances were measured with a photometer (Model IL 1700; International Light, Newburyport, MA).

2.3. Focal ERG recordings

The cornea was anesthetized with topical 1% tetracaine, and the pupils were dilated with topical 0.5% tropicamide and 0.5% phenylephrine HCl. The ERGs were recorded with a Burian-Allen bipolar contact lens electrode (Hansen Ophthalmic Development Laboratories, Iowa City, IA), and the ground electrode was attached to the ipsilateral ear. The responses were amplified, and the band pass filters were set at 0.5 to 1000 Hz. The ERGs were digitized at 5 kHz, and 500 responses were averaged (MEB-9100 Neuropack; Nihon Kohden, Tokyo, Japan).

To confirm that the stimulus and recording conditions elicited focal ERGs, we investigated the effect of stray light on the responses. We made an approximately 15° laser scar on the visual streak to two other WT pigmented rabbits (Fig. 1A), and we recorded the focal ERGs elicited by stimulating the visual streak and the photocoagulated area.

A fundus photograph of a 3-months-old WT rabbit is shown in Fig. 2, and the gray ellipse shown below the optic disc outlines the

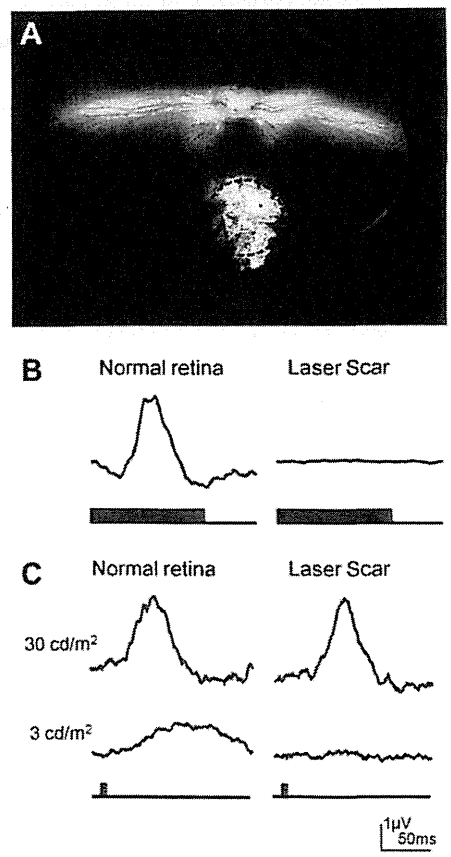

Fig. 1. Experiments to determine whether the focal ERGs arise from only the stimulated area. (A) Fundus photograph showing laser scar in the visual streak of a wild rabbit. Dotted circular indicates the area of stimulation to elicit focal ERGs. (B) Focal cone ERGs from normal retina (visual streak) and laser scar ERGs were recorded with a 3 cd/m^2 steady background. The luminance of the stimulus spot was 30 phot cd/m^2, and the stimulus duration was 100 ms. The focal ERGs were almost non-recordable from the area photocoagulated. (C) Focal rod ERGs from normal retina (visual streak) and laser scar. ERGs were recorded without background light. The ERGs recorded with stimulus intensity of 30 cd/m^2 with 10 ms duration are shown in the upper row. ERGs were recorded even from the area photocoagulated due to stray light. The ERGs recorded with stimulus intensity of 3 cd/m^2 with 10 ms duration are shown in the lower row. The focal ERGs were almost non-recordable from the area photocoagulated.

visual streak (Famiglietti & Sharpe, 1995; Juliusson et al., 1994). To compare the local retinal function of Tg and WT rabbits, we recorded ERGs from 5 areas of the retina as shown in Fig. 2. The ERGs were elicited by a 15° stimulus spot placed superior to the disc (A), nasal to the visual streak (B), center of the visual streak (C), temporal to the visual streak (D), and inferior to the visual streak (E).

2.4. Measurement of b-wave and OPs

The amplitudes of the b-waves and OPs were measured by a masked researcher. The amplitude of the b-wave was measured from the bottom of the negative a-wave to the top of the positive wave (Fig. 2, lower). To determine the appropriate band pass filters for isolating the OPs of WT and Tg rabbits, we first analyzed the ERGs by Fast Fourier Transform (FFT) as reported (Sakai et al., 2009). Based on the results, we chose band pass settings of 50–300 Hz for isolating the focal OPs (Fig. 2, lower). We measured the amplitude of each OP wavelet from the trough to the peak of the filtered waveforms, and one masked researcher checked the original waveform and decided on the position of the trough and peak of each OP. When a clear oscillation could not be found, we

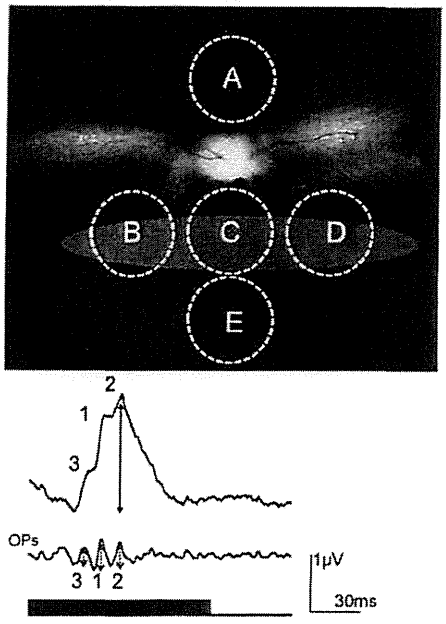

Fig. 2. Fundus panorama of left eye of a 3-months-old WT rabbit (upper). White ellipse inferior to the optic disc indicates the location of the visual streak. We recorded focal ERGs using a 15° stimulus spots from the 5 areas. (A) Superior to the optic disc. (B) Nasal on the visual streak. (C) Center of visual streak. (D) Temporal on the visual streak. (E) Ventral of the visual streak. Representative focal ERGs of WT rabbit (lower). Upper trace is the original waveform and the extracted OPs are in the middle. Stimulus markers are at the bottom. Arrow in the original wave shows the amplitude of the b-wave. The OPs consists of several wavelets; 1 is the largest OP, 2 is the second largest, and 3 is the third largest. We analyzed the sum of the amplitudes of 1, 2, and 3.

set the amplitude to zero. We used the sum of the 3 largest OP wavelets (1, 2, and 3) because each OP was too small to analyze separately.

2.5. Retinal histology

To examine the histological changes of the retina, 3 eyes of 6-months-old Tg and WT rabbits were evaluated. The rabbit eyes were fixed overnight in a mixture of 10% neutral buffered formalin and 2.5% glutaraldehyde then transferred to 10% neutral buffered formalin. The tissues were trimmed, embedded in paraffin, sectioned vertically through the optic nerve (superior-inferior), and stained with hematoxylin and eosin. Retinal sites 4 mm superior to the optic disc, 2 mm and 6 mm inferior to the optic disc were evaluated. These sites were presumed to be the center of the focal ERG stimulus at the superior, center, and inferior to the optic disc (Fig. 2 upper). The thickness of the inner retina from the inner limiting membrane to the outer plexiform layer, and the outer nuclear layer (ONL) was measured.

2.6. Statistical analyses

The data were analyzed with the SPSS computer software. The amplitude of the b-wave and sum OPs were compared with *t*-tests or multiple comparisons. A difference was considered statistically significant when $P < 0.05$.

3. Results

3.1. Assessing recording conditions

To confirm that our focal ERGs were responses only from the stimulated site of the retina and not from other sites stimulated by stray light, we made an approximately 15° laser scar on the visual streak of two WT rabbits (Fig. 1A). We then recorded focal ERGs from the normal visual streak and from the area of the laser photocoagulation with a 15° spot under both photopic and scotopic conditions. We determined the appropriate stimulus conditions for recording focal ERG for WT rabbits initially. For the photopic condition, we used a stimulus with a luminance of 30 cd/m^2 with 100 ms duration presented on a 3 cd/m^2 steady background. We found that the focal ERGs from laser scar were below the noise level of the recordings (Fig. 1B) and concluded this stimulus setting was appropriate for recording focal cone ERGs. Next we determined the conditions for recording focal rod ERGs. We found that stimuli of 30 cd/m^2 with 10 ms duration imaged on the laser scar elicited ERGs after 15 min dark-adaptation. We assumed that the responses originated from stray light (Fig. 1C), and we reduced the stimulus intensity and found that stimulus intensity of 3 cd/m^2 and 10 ms duration did not elicit a response when it was imaged on the laser scar. We then used these stimulus parameters to study the focal rod ERGs (Fig. 1C).

3.2. Focal cone ERGs from wild type (WT) rabbits

Focal cone ERGs were recorded from the 5 retinal areas of 6 WT rabbits at 3 and 6 months. Representative focal cone ERGs elicited from areas A to E of a 3-months-old WT rabbit are shown in the left row of Fig. 3. The isolated OPs are shown below each of the ERGs. The focal cone ERGs from each site were similar in shape and consisted of a small negative a-wave followed by a large positive b-wave with the OPs superimposed on the b-wave. The mean ± SEM amplitudes of the b-waves of the focal ERGs at 3 and 6 months are plotted on the left side of Fig. 4 (black bars). At 3 months, the b-wave of area C was significantly larger than that of areas A and E ($C = 3.1 \pm 1.0$ μV; $A = 2.3 \pm 1.2$ μV; $E = 2.3 \pm 1.0$ μV; $P < 0.05$; paired *t*-tests). The means ± SEM amplitudes of the sum of the OPs at 3 and 6 months WT rabbits ($n = 6$ each) are plotted on the right side of Fig. 4. The amplitudes of the OPs varied considerably among the rabbits, and the differences in the amplitudes among the 5 areas (minimum = 0.7 ± 0.1 μV at B; maximum = 1.1 ± 0.2 μV at A at 3 months; multiple comparisons) were not significant. We also compared the focal cone ERGs of 3- and 6-months-old WT rabbits. The amplitudes of the b-waves from each area of 6-months-old WT rabbit was slightly smaller than that of 3–months-old rabbits, but the differences between the amplitudes at the two ages in each area were not significant (paired *t*-tests).

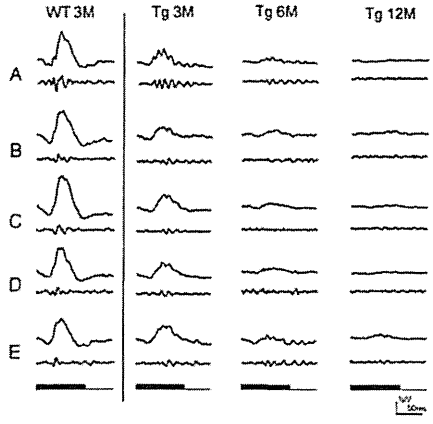

Fig. 3. Representative focal cone ERGs recorded from the 5 areas designated in Fig. 2. For ERGs of a WT rabbit at 3 months and of Tg rabbits at 3, 6, and 12 months are shown. The focal cone ERGs of the Tg rabbits decreases with increasing age. The OPs from area A is larger than those from other areas in the 3-months-old Tg rabbit.

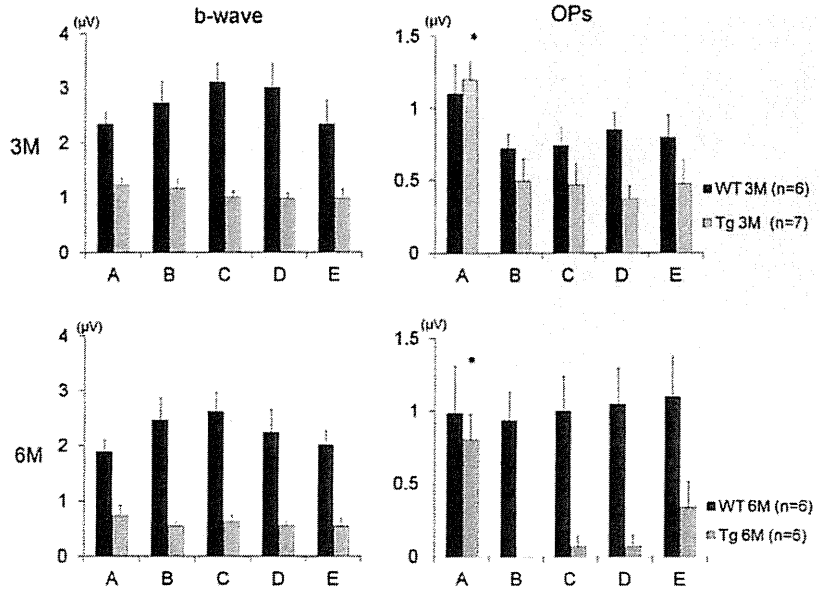

Fig. 4. Amplitudes of b-wave and OPs from 5 areas of WT and Tg rabbits (mean + SEM). Amplitudes of focal ERG b-wave at 3-months-old are shown in the upper left, and the sum of focal ERG OPs at 3-months-old are shown in the upper right. Amplitudes of the focal ERG b-waves at 6-months-old are shown in the lower left, and the amplitudes of sum of focal ERG OPs at 6-months-old are shown in the lower right. The amplitude of OPs in area A was significantly larger than that in other areas in Tg rabbit (*$P < 0.05$).

3.3. Focal cone ERGs of Tg rabbits

Focal cone ERGs were recorded from 7 Tg rabbits at 3 months, 6 Tg rabbit at 6 months and 3 Tg rabbits at 12 months. Representative ERGs of one Tg rabbit recorded at 3, 6, and 12 months are shown in Fig. 3. The amplitudes of the ERGs progressively decreased with increasing age and were almost non-recordable at 12 months. The OPs from the superior area (A) were distinguishable at 3 months. The amplitudes of b-waves in the Tg rabbits were significantly smaller than that of WT rabbits at each recording area (Fig. 4 left, gray bars). The means ± SEMs of the amplitude of the b-waves at 6 months were significantly reduced in area A (0.7 ± 0.2 μV), area B (0.6 ± 0.1 μV), area C (0.6 ± 0.1 μV), area D (0.6 ± 0.1 μV), and area E (0.6 ± 0.2 μV) than that at 3 months (A = 1.2 ± 0.1 μV; B = 1.2 ± 0.2 μV; C = 1.0 ± 0.1 μV; D = 1.0 ± 0.1 μV; E = 1. 0 ± 0.2 μV; $P < 0.05$, *t*-tests for all areas). However, the differences in the amplitudes of the b-waves in the 5 areas were not significant at 3 and 6 months.

At 3 months, the amplitudes of the OPs were better preserved than the b-waves, and the OPs/b-wave ratio was higher than that in WT rabbits at every recording area. The sum of the OPs at area A (1.2 ± 0.1 μV) was best preserved, and the sum was significantly larger than that of other areas (B = 0.5 ± 0.2 μV; C = 0.5 ± 0.2 μV; D = 0.4 ± 0.1 μV; E = 0.5 ± 0.2 μV; $P < 0.05$, multiple analyses; Fig. 4). At 6 months, the OPs became undetectable in most of the Tg rabbits at areas B, C, and D. However at area A, the OPs were still prominent, and the amplitude was significantly larger than that at the other recording areas (0.8 ± 0.2 μV; $P < 0.05$, multiple analysis). At 12 months, the focal cone ERGs of the 3 Tg rabbits became almost non-recordable at all sites.

3.4. Focal rod ERGs of WT and Tg rabbits

Focal rod ERGs were recorded from the 5 retinal areas of 2 Tg and 2 WT rabbits at 3 months. Representative ERGs from a Tg and a WT rabbit are shown in Fig. 5. The focal rod ERGs from each site were similar in shape which had small positive b-wave but no a-wave and OPs. The amplitudes of b-wave of WT rabbit were approximately 1.2 μV at all 5 areas. On the other hand, the focal rod ERGs of Tg rabbit were non-recordable even at 3 months.

3.5. Retinal histology

The retinal sections of the area of superior to disc (A), center of the visual streak (C), ventral of visual streak (E) of a WT rabbit and a Tg rabbit at 6 months are shown in the upper half of Fig. 6. It is known that in normal rabbits, the density of rods and cones is highest at the visual streak. Consistent with previous reports (Famiglietti & Sharpe, 1995), the thickness of the ONL in WT rabbits was maximum at the visual streak (Fig. 6 lower right). There were regional differences in the degree of photoreceptor loss in the Tg rabbits (Kondo et al., 2009). Only a single row of nuclei remained in the ONL at the center of the visual streak (C) and the thickness of the ONL at the visual streak was reduced relatively more than the two other locations (Fig. 6 lower right). In contrast, the thickness of the inner retina was well preserved at 6 months. The thickness of inner retina was almost same as that of control. From retinal histology of hematoxylin and eosin stained retinas, it was difficult to detect any inner retinal change which could have caused the abnormal OPs responses dorsal to the disc (A).

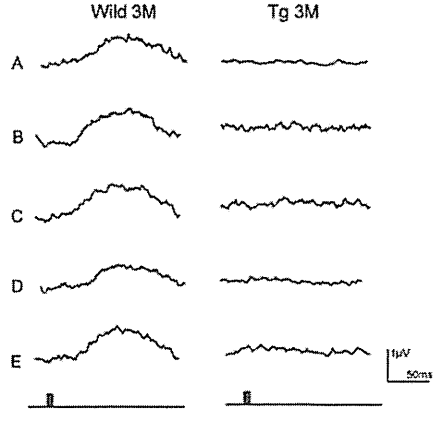

Fig. 5. Representative focal rod ERGs recorded from the 5 areas designated in Fig. 2. ERGs of a WT and a Tg rabbit at 3 months are shown. The focal rod ERGs of the Tg rabbit were non-recordable at 3 months.

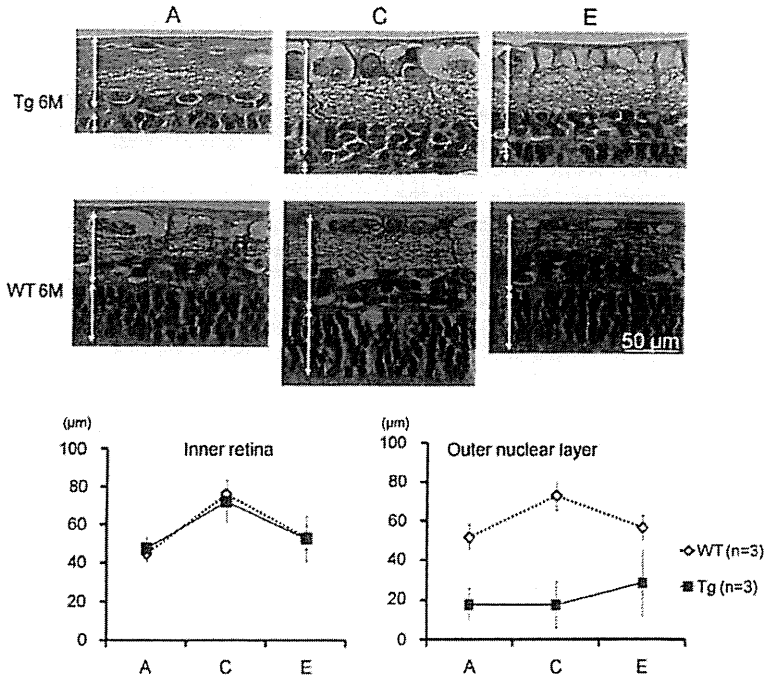

Fig. 6. Retinal histology of Tg rabbits. Vertical retinal sections from 4 mm superior to the optic nerve head (A), 2 mm (C) and 6 mm (E) inferior to the optic nerve head of 6-months-old WT and Tg rabbits are shown in the upper half. White two way arrows in the micrograph indicate thickness of inner retina and outer nuclear layer (ONL) respectively. Thickness of the inner retina and ONL along the vertical meridian measured at 3 retinal locations are shown in the lower. Mean ± SD of 3 WT and 3 Tg rabbits are plotted.

4. Discussion

We recorded focal ERGs from 5 retinal areas of Tg rabbits during the course of retinal degeneration. Our previous study indicated the Tg rabbits had a progressive dysfunction of the rods (Kondo et al., 2009). Because focal ERGs recorded under scotopic conditions are non-recordable at 3 months, we were not able to evaluate local rod function in Tg rabbit. The amplitudes of the focal cone ERG b-waves became progressively smaller with increasing age in all regions, and there were no differences in the amplitudes from the 5 areas. On the other hand, the amplitudes of the summed OPs had regional variations with that of the superior retina (area A) significantly larger than that from other areas at both 3 and 6 months.

4.1. Focal ERGs from WT rabbits

The characteristics of the multifocal ERGs (mfERGs) of normal rabbits or Tg rabbits have been determined (Horiguchi et al., 1998; Wallenten, Andreasson, & Ghosh, 2008; Yokoyama et al., 2010). However to the best of our knowledge, this is the first report of focal ERGs recorded from Tg rabbits. The waveforms of mfERGs are derived from mathematical modeling of the potential changes of the retinal neurons (Sutter & Tran, 1992), while the waveforms of focal ERGs are the potential changes of the retinal neurons. Our laboratory has studied focal ERGs of humans and monkeys using this technique for more than twenty years (Miyake, 1990; Miyake et al., 1989; Shiroyama & Miyake, 1990). Monitoring the fundus during the recording was essential because the animals cannot fixate a target, and thus we believe that our system is a more appropriate method of recording ERGs from localized areas than mfERGs.

The focal cone ERGs of rabbits at light on consisted of a- and b-waves with OPs as in primates (Kondo et al., 2008; Miyake et al., 1989). When the light is turned off, a d-wave appeared in the primate ERGs but was barely detected in rabbits. The amplitude of the focal cone ERGs from the fovea in human is about 5 μV, while that from the visual streak of rabbits was about 3 μV. This lower amplitude may be because the cone density is higher in humans. Comparing the five retinal areas, the b-wave amplitudes from the visual streak (B–D) was larger than that of two other areas (A and E). These results are comparable to histological data that show that the cone density is highest in the visual streak (Famiglietti & Sharpe, 1995; Juliusson et al., 1994). For the focal rod ERGs of WT rabbits, the waveforms and amplitudes were not different among the different retinal areas. In addition, the waveforms were similar to those of the full-field rod responses elicited with weak stimuli under dark-adapted conditions (Marmor et al., 2009). These results indicate that the rod function is not significantly different in the regions tested.

4.2. Focal ERGs from Tg rabbits

We followed the changes in the amplitudes of the focal cone ERGs during the course of retinal degeneration in Tg rabbit. Earlier studies reported that reductions in the mfERG amplitudes of mice, cats, pigs, and rabbits with genetically-induced retinal degeneration (Ng et al., 2008; Seeliger & Narfstrom, 2000; Seeliger et al., 2003; Yokoyama et al., 2010). However, the OPs of the mfERGs could not be analyzed. Because the OPs originate mainly from the inner retina, it is reasonable to analyze the OPs to determine whether functional changes of the inner retinal neurons are present in Tg rabbits.

Earlier, we reported that the thickness of the outer nuclear layer in the visual streak of albino Tg rabbits was one-half of that of WT at 3 months and one-third of that of WT rabbits at 6 months (Kondo et al., 2009). These results are comparable with our focal cone ERG results; the amplitude of the b-waves of the focal cone ERGs was one-third of WT rabbit at 3 months, one-fourth of that at 6 months, and non-recordable at 12 months. We also reported that the loss of photoreceptors in the visual streak was more severe than that at 6 mm superior to the optic nerve head (ONH) and 8 mm inferior to the ONH. However, we did not find distinct regional differences in the amplitudes of the b-waves of the focal cone

ERGs probably because the amplitude of the focal ERGs was small and the signal-to-noise ratio was too large to detect the differences. Our focal cone ERGs might be less sensitive in detecting regional differences than histopathological analyses.

We have reported the change of the full-field cone ERGs in Tg rabbit in earlier studies (Hirota et al., 2012; Kondo et al., 2008; Sakai et al., 2009). However, the focal ERGs results contradict our earlier findings that there was no significant difference in the amplitude of the full-field cone b-wave V_{max} between Tg and Wt rabbits even at 12 months (see Fig. 3 and Table 1 in Sakai et al., 2009). We also reported that the half-saturation coefficient (K) was already reduced significantly at 3 months (Sakai et al., 2009). These findings suggest that dimmer flashes can detect the differences between Tg and WT rabbits more easily. In addition, slight degeneration of the photoreceptors would not affect coneERG b-wave amplitudes elicited by high intensity stimuli because the b-wave amplitudes are at the saturated level. Our focal cone ERGs were recorded with relatively dim stimulus (30 cd/m^2) to avoid stray light effects and our system seemed to be more suitable for detecting functional loss due to photoreceptor degeneration.

An interesting finding in this study was that the amplitudes of the OPs were better preserved than the b-waves and the OPs/b-wave ratio was greater than that in WT rabbits at every recording area at 3 months. In addition, the sum of the OPs at area A was best preserved, and the sum was significantly larger than that of other areas. We have reported that the OPs of the full-field cone ERGs of 3-month-old Tg rabbit were 1.7 times larger than that of WT rabbits (Sakai et al., 2009). We suggest that secondary functional changes in the inner retinal neurons, retinal ganglion cells, and/or amacrine cells, caused this phenomenon because these OPs were TTX sensitive (Sakai et al., 2009). Although the amplitudes of the OPs were not supernormal even at area A, our results suggest there are regional differences in secondary functional alterations in the inner retinal neurons after photoreceptor death. When we compared the histology of the dorsal, visual streak, and ventral retina from 6-months-old rabbit in hematoxylin and eosin stained sections, we were not able to find differences in the thickness of the inner retina. A previous OCT study showed that the inner nuclear layer (INL) thickness in RP rabbits did not differ from that of WT rabbits (Muraoka et al., 2012). To explore the mechanisms of large OPs at ventral site, we will need to evaluate the regional differences of the inner retinal histopathology more precisely in the future.

We reported that the OPs of the focal macular ERGs of RP patients were better preserved than the a- and b-waves (Ikenoya et al., 2007). These data raise the possibility that similar secondary functional changes can occur in some RP patients.

Finally, we believe that this Tg rabbit will serve as a useful mid-sized animal model with which to develop treatments including cell transplantation (MacLaren et al., 2006) and retinal prosthesis (Nishida et al., 2010; Weiland, Liu, & Humayun, 2005).

Acknowledgments

We thank Prof. Duco I. Hamasaki for editing the manuscript.

Grant Support: 20592075 (M.K.) and 25462709 (S.U.) from the Ministry of Education, Science, Sports and Culture, Japan.

References

Chan, H. L., & Brown, B. (1998). Investigation of retinitis pigmentosa using the multifocal electroretinogram. *Ophthalmic and Physiological Optics, 18*(4), 335–350.

Dong, C. J., Agey, P., & Hare, W. A. (2004). Origins of the electroretinogram oscillatory potentials in the rabbit retina. *Visual Neuroscience, 21*(4), 533–543.

Famiglietti, E. V., & Sharpe, S. J. (1995). Regional topography of rod and immunocytochemically characterized "blue" and "green" cone photoreceptors in rabbit retina. *Visual Neuroscience, 12*(6), 1151–1175.

Heckenlively, J. R. (1988). *Retinitis pigmentosa*. JB Lippincott, Philadelphia (pp. 221–252).

Hirota, R., Kondo, M., Ueno, S., Sakai, T., Koyasu, T., & Terasaki, H. (2012). Photoreceptor and post-photoreceptoral contributions to photopic ERG a-wave in rhodopsin P347L transgenic rabbits. *Investigative Ophthalmol and Visual Science, 53*(3), 1467–1472.

Hood, D. C., Holopigian, K., Greenstein, V., Seiple, W., Li, J., Sutter, E. E., et al. (1998). Assessment of local retinal function in patients with retinitis pigmentosa using the multi-focal ERG technique. *Vision Research, 38*(1), 163–179.

Horiguchi, M., Suzuki, S., Kondo, M., Tanikawa, A., & Miyake, Y. (1998). Effect of glutamate analogues and inhibitory neurotransmitters on the electroretinograms elicited by random sequence stimuli in rabbits. *Investigative Ophthalmology & Visual Science, 39*(11), 2171–2176.

Ikenoya, K., Kondo, M., Piao, C. H., Kachi, S., Miyake, Y., & Terasaki, H. (2007). Preservation of macular oscillatory potentials in eyes of patients with retinitis pigmentosa and normal visual acuity. *Investigative Ophthalmology & Visual Science, 48*(7), 3312–3317.

Juliusson, B., Bergstrom, A., Rohlich, P., Ehinger, B., van Veen, T., & Szel, A. (1994). Complementary cone fields of the rabbit retina. *Investigative Ophthalmology & Visual Science, 35*(3), 811–818.

Kondo, M., Sakai, T., Komeima, K., Kurimoto, Y., Ueno, S., Nishizawa, Y., et al. (2009). Generation of a transgenic rabbit model of retinal degeneration. *Investigative Ophthalmology & Visual Science, 50*(3), 1371–1377.

Kondo, M., Ueno, S., Piao, C. H., Miyake, Y., & Terasaki, H. (2008). Comparison of focal macular cone ERGs in complete-type congenital stationary night blindness and APB-treated monkeys. *Vision Research, 48*(2), 273–280.

MacLaren, R. E., Pearson, R. A., MacNeil, A., Douglas, R. H., Salt, T. E., Akimoto, M., et al. (2006). Retinal repair by transplantation of photoreceptor precursors. *Nature, 444*(7116), 203–207.

Marc, R. E., Jones, B. W., Anderson, J. R., Kinard, K., Marshak, D. W., Wilson, J. H., et al. (2007). Neural reprogramming in retinal degeneration. *Investigative Ophthalmology & Visual Science, 48*(7), 3364–3371.

Marmor, M. F., Fulton, A. B., Holder, G. E., Miyake, Y., Brigell, M., & Bach, M. (2009). ISCEV Standard for full-field clinical electroretinography (2008 update). *Documenta Ophthalmologica, 118*(1), 69–77.

Miyake, Y. (1990). Macular oscillatory potentials in humans. Macular OPs. *Documenta Ophthalmologica, 75*(2), 111–124.

Miyake, Y., Shiroyama, N., Horiguchi, M., & Ota, I. (1989). Asymmetry of focal ERG in human macular region. *Investigative Ophthalmology & Visual Science, 30*(8), 1743–1749.

Muraoka, Y., Ikeda, H. O., Nakano, N., Hangai, M., Toda, Y., Okamoto-Furuta, K., et al. (2012). Real-time imaging of rabbit retina with retinal degeneration by using spectral-domain optical coherence tomography. *PLoS One, 7*(4), e36135.

Ng, Y. F., Chan, H. H., Chu, P. H., To, C. H., Gilger, B. C., Petters, R. M., et al. (2008). Multifocal electroretinogram in rhodopsin P347L transgenic pigs. *Investigative Ophthalmology & Visual Science, 49*(5), 2208–2215.

Nishida, K., Kamei, M., Kondo, M., Sakaguchi, H., Suzuki, M., Fujikado, T., et al. (2010). Efficacy of suprachoroidal–transretinal stimulation in a rabbit model of retinal degeneration. *Investigative Ophthalmology & Visual Science, 51*(4), 2263–2268.

Sakai, T., Kondo, M., Ueno, S., Koyasu, T., Komeima, K., & Terasaki, H. (2009). Supernormal ERG oscillatory potentials in transgenic rabbit with rhodopsin P347L mutation and retinal degeneration. *Investigative Ophthalmology and Visual Science, 50*(9), 4402–4409.

Seeliger, M. W., Kretschmann, U. H., Apfelstedt-Sylla, E., & Zrenner, E. (1998). Implicit time topography of multifocal electroretinograms. *Investigative Ophthalmology & Visual Science, 39*(5), 718–723.

Seeliger, M. W., & Narfstrom, K. (2000). Functional assessment of the regional distribution of disease in a cat model of hereditary retinal degeneration. *Investigative Ophthalmology & Visual Science, 41*(7), 1998–2005.

Seeliger, M. W., Weber, B. H., Besch, D., Zrenner, E., Schrewe, H., & Mayser, H. (2003). MfERG waveform characteristics in the RS1h mouse model featuring a 'negative' ERG. *Documenta Ophthalmologica, 107*(1), 37–44.

Shiroyama, N., & Miyake, Y. (1990). Analysis of focal macular ERG in idiopathic central serous chorioretinopathy. *Nippon Ganka Gakkai Zasshi, 94*(11), 1048–1056.

Sugita, T., Kondo, M., Piao, C. H., Ito, Y., & Terasaki, H. (2008). Correlation between macular volume and focal macular electroretinogram in patients with retinitis pigmentosa. *Investigative Ophthalmology & Visual Science, 49*(8), 3551–3558.

Sutter, E. E., & Tran, D. (1992). The field topography of ERG components in man – I. The photopic luminance response. *Vision Research, 32*(3), 433–446.

Vajaranant, T. S., Seiple, W., Szlyk, J. P., & Fishman, G. A. (2002). Detection using the multifocal electroretinogram of mosaic retinal dysfunction in carriers of X-linked retinitis pigmentosa. *Ophthalmology, 109*(3), 560–568.

Wachtmeister, L. (1998). Oscillatory potentials in the retina: What do they reveal. *Progress in Retinal and Eye Research, 17*(4), 485–521.

Wallenten, K. G., Andreasson, S., & Ghosh, F. (2008). Retinal function after vitrectomy. *Retina, 28*(4), 558–563.

Weiland, J. D., Liu, W., & Humayun, M. S. (2005). Retinal prosthesis. *Annual Review of Biomedical Engineering, 7*, 361–401.

Weleber, R. G., and Gregory-Evance, K., (2006). *Retinitis pigmentosa and allied disorders* (4th ed.). Retina 1 (Mosby St. Louis. Basic Science and Inherited Retinal Disease).

Yokoyama, D., Machida, S., Kondo, M., Terasaki, H., Nishimura, T., & Kurosaka, D. (2010). Pharmacological dissection of multifocal electroretinograms of rabbits with Pro347Leu rhodopsin mutation. *Japanese Journal of Ophthalmology, 54*(5), 458–466.

Eye (2013) 27, 871–877

www.nature.com/eye

CLINICAL STUDY

Displacement of foveal area toward optic disc after macular hole surgery with internal limiting membrane peeling

K Kawano[1], Y Ito[1], M Kondo[1,2], K Ishikawa[1], S Kachi[1], S Ueno[1], Y Iguchi[1] and H Terasaki[1]

Abstract

Purpose To determine whether there is a displacement of the fovea toward the optic disc after successful macular hole (MH) surgery with internal limiting membrane (ILM) peeling.

Methods The medical records of 54 eyes of 53 patients that had undergone pars plana vitrectomy with ILM peeling and gas or air tamponade for an idiopathic MH were evaluated. Spectral-domain optical coherence tomography (OCT) had been performed before and >6 months after the surgery. The preoperative distances between the center of the MH and the optic disc (MH-OD), center of the MH and the bifurcation or crossing of retinal vessels (MH-RV) were measured in the OCT images. In addition, the postoperative distance between the center of the fovea and optic disc (F-OD) and the center of the fovea and the same bifurcation or crossing of retinal vessels (F-RV) were measured in the OCT images.

Results The F-OD was 2.67 ± 0.33 disc diameters (DD), which was significantly shorter than that of the MH-OD of 2.77 ± 0.33 DD ($P<0.001$). The F-RV was also significantly shorter than the MH-RV on the inner nasal area (from 0.85 ± 0.16DD to 0.79 ± 0.15DD; $P<0.001$), the inner temporal area (from 0.82 ± 0.15DD to 0.77 ± 0.14DD; $P<0.001$), and outer nasal area (from 1.70 ± 0.31DD to 1.65 ± 0.32DD; $P<0.001$), but it was significantly longer than the MH-RV in the outer temporal area (from 1.65 ± 0.29DD to 1.68 ± 0.29DD; $P<0.001$).

Conclusion Our results showed that successful closure of a MH by vitrectomy with ILM peeling and gas tamponade leads to a displacement of the center of the macula toward the optic disc.

Eye (2013) 27, 871–877; doi:10.1038/eye.2013.99; published online 24 May 2013

Keywords: macular hole; vitrectomy; internal limiting membrane peeling; displacement of fovea

Introduction

An idiopathic macular hole (MH) can be successfully closed by vitrectomy,[1–6] and the success rate is improved if the internal limiting membrane (ILM) is peeled during the vitrectomy.[2–6] Although the mechanism causing the MH has been essentially determined,[7–12] the mechanism for the MH closure has not been definitively determined.

Yanagita *et al*[13] reported that after a closure of a MH by vitrectomy, the retinal blood vessels near the MH are displaced toward the center of the fovea in all cases. They suggested that the retina around the MH moved toward the foveal pit after vitrectomy. On the other hand, we have noted that in many cases the retinal vessels in the macular area appeared to move toward the optic disc after vitrectomy that successfully closed a MH.

Thus, the purpose of this study was to test the hypothesis that the center of the macular area moves nasally toward the optic disc after successful closure of a MH by vitrectomy with ILM peeling.

[1]Department of Ophthalmology, Nagoya University School of Medicine, Nagoya, Japan

[2]Department of Ophthalmology, Mie University School of Medicine, Tsu, Japan

Correspondence:
Y Ito, Department of Ophthalmology, Nagoya University School of Medicine, 65 Tsuruma-cho, Showa-ku, Nagoya, Aichi 466-8550, Japan.
Tel: +81 5 2744 2271;
Fax: +81 5 2744 2279.
E-mail: yasu@med.nagoya-u.ac.jp

Received: 17 December 2012
Accepted in revised form: 23 April 2013
Published online: 24 May 2013

Meeting Presentation: Parts of this study were presented at the Japanese Clinical Ophthalmological Society Meeting, October 2011, and the Japanese Ophthalmological Society Meeting, May 2012.

Materials and methods

Study population

We reviewed the medical charts of 54 eyes of 53 patients who underwent successful vitrectomy for an idiopathic MH at the Nagoya University Hospital between October 2008 and May 2012. There were 33 women and 20 men. The mean ± SD of the age was 65.3 ± 6.0 years with a range of 54–78 years. There were 25 stage-2 MHs (46%), 12 stage-3 MHs (22%), and 17 stage-4 MHs (31%).[7] All MHs were closed after a single surgery.

Eyes excluded from the statistical analyses were those with a reopening of the MH, with high myopia, or with a retinal detachment combined with the MH. Eyes with other macular diseases, such as age-related macular degeneration, were also excluded.

We also reviewed the charts of five eyes of five patients who had an idiopathic MH that closed spontaneously. The measurements made on these five eyes were identical to that of eyes that underwent vitrectomy.

The protocol for this study was approved by the institutional review board of the Nagoya University School of Medicine, and the procedures used conformed to the tenets of the Declaration of Helsinki.

Surgical techniques

A three-port pars plana vitrectomy with ILM peeling was carried out with 23- or 25-gauge instruments in all cases. All of the patients underwent combined cataract surgery except one patient who was pseudophakic. Triamcinolone acetonide was used for staining the ILM in all 54 eyes. The area of ILM peeling was symmetrical around the fovea and was about four disc diameters (DD). Sulfur hexafluoride (0.5–1.0 ml) gas was used in 38 eyes, perfluoropropane (0.5–0.8 ml) gas in 15 eyes, and simple fluid gas exchange without any gas injection was used in one eye as a tamponade. The patients were instructed to maintain a face-down position as much as possible until the closure of MHs was confirmed by OCT.

Examination and measurement procedures

All patients underwent a complete ophthalmic examination, including measurements of the best-corrected visual acuity (BCVA), slit-lamp biomicroscopy, fundus examination, and optical coherence tomography (OCT; Cirrus OCT; Carl Zeiss Meditec, Dublin, CA, USA) before and 1–2 weeks, 1–3 months, and >6 months after the vitrectomy. Axial length was measured in all eyes preoperatively (IOL master, Carl Zeiss Meditec). The fovea was scanned with the 200 × 200 Macular Cube protocol of the Cirrus HD-OCT. OCT images were excluded if the eye moved during the scans.

The distance across the fundus was measured in the Cirrus OCT images.[14] The Cirrus OCT instrument allows a direct registration of the OCT projection maps onto the infrared line scanning ophthalmoscopic image. The location of the center of the MH or postoperative foveola was determined by realigning the vertical and horizontal OCT scans in the analysis window manually (Figures 1a, b, d and e). In cases where the postoperative foveal pit was irregular, center of fovea was considered to be the thinnest part in the OCT image. In cases where the postoperative foveal pit was flat, the center of the fovea was considered to be the center of foveal pit.

The preoperative distance between center of MH and optic disc (MH-OD) and the distance between center of the MH and a bifurcation or crossing of retina vessels (MH-RV) were measured in the Cirrus OCT images (Figure 1c). In the same way, the postoperative distance between the fovea and optic disc (F-OD), and the distance between the fovea and a bifurcation or crossing of retina vessels (F-RV) were measured in the Cirrus OCT images. Each distance was measured manually with the caliper function embedded in the OCT instrument. To compensate for variations in the magnification of each scan, each distance was divided by vertical diameter of the optic disc, and the distance was expressed in DD units.

The locations of the bifurcation or crossing of the retinal vessels were selected in four areas: the inner nasal area, the inner temporal area, the outer nasal area, and the outer temporal area (Figure 1c). The inner areas were within a circle of two DD centered on the fovea, and the outer area was between circles of two and four DDs centered on fovea. The margin between the nasal and temporal areas was a vertical line passing through the fovea. The movement of the macula in each area was analyzed separately.

Eyes with spontaneous closure of MH

The MHs of five eyes closed spontaneously, and both the pre-closure and post-closure OCT images were available. The measurements of the displacement were done identically to the eyes that underwent vitrectomy. The mean ± SD age of these three women and two men was 65.6 ± 6.7 years with a range of 56–73 years. There were two stage-2 MHs (40%) and three stage-3 MHs (60%).

Statistical analyses

The significance of the differences between the pre- and postoperative values was determined by paired *t*-tests, and single and stepwise regression analysis was used to determine the parameters that were significantly associated with the distance of movement of the fovea (PASW statistics version 18.0; SPSS Inc and IBM

Company, Chicago, IL, USA). A $P<0.05$ was taken to be statistically significant.

Results

The pre- and postoperative OCT images of 36 eyes of 36 patients at 1–3 months and >6 months were of sufficient quality to be analyzed. The mean ± SD preoperative MH-OD distance was 2.77 ± 0.33 DD with a range of 2.08–3.47 DD. The mean postoperative F-OD distance was 2.67 ± 0.32 DD with a range of 2.05–3.34 DD at 1–3 months, and 2.67 ± 0.33 DD with a range of 2.03–3.37 DD at >6 months. The F-OD distance at 1–3 and >6 months after surgery were significantly shorter than the MH-OD by 3.3 ± 2.0% and 3.6% ± 1.8%, respectively, (both $P<0.001$, paired *t*-tests).

The OCT images of 13 eyes that were recorded within 2 weeks after surgery and were good enough to be analyzed were available. In these 13 eyes, the average MH-OD distance was 2.61 ± 0.16 DD, and the F-OD distance was 2.57 ± 0.18 DD at 1–2 weeks, 2.54 ± 0.16 DD at 1–3 months, and 2.53 ± 0.16 DD at >6 months after the vitrectomy. The F-OD distance at 1–2 weeks, 1–3 months, and >6 months after surgery were significantly shorter than the MH-OD distance by 1.8% ± 1.5% ($P=0.001$, paired *t*-test), by 2.9 ± 1.4% ($P<0.001$, paired *t*-test), and by 3.1% ± 1.5% ($P<0.001$, paired *t*-test; Figure 2a).

The mean ± SD of the MH-RV distance in the inner nasal area for the 36 eyes was 0.85 ± 0.16 DD preoperatively. The mean ± SD of the F-RV distance in the inner nasal area was 0.80 ± 0.16 DD at 1–3 months after surgery and 0.79 ± 0.15 DD at >6 months after the vitrectomy. The F-RV distance in the inner nasal area were significantly shorter than the MH-RV distance by 6.6 ± 4.4% ($P<0.001$, paired *t*-test) at 1–3 months and by 7.2% ± 4.1% ($P<0.001$, paired *t*-test) at 6 months after the vitrectomy (Figure 3).

The mean ± SD of the MH-RV distance in the inner temporal area was 0.82 ± 0.15 DD preoperatively. The mean of the F-RV distance in the inner temporal area was 0.77 ± 0.15 DD at 1–3 months after surgery and 0.77 ± 0.14 DD at >6 months after the vitrectomy. The F-RV distance

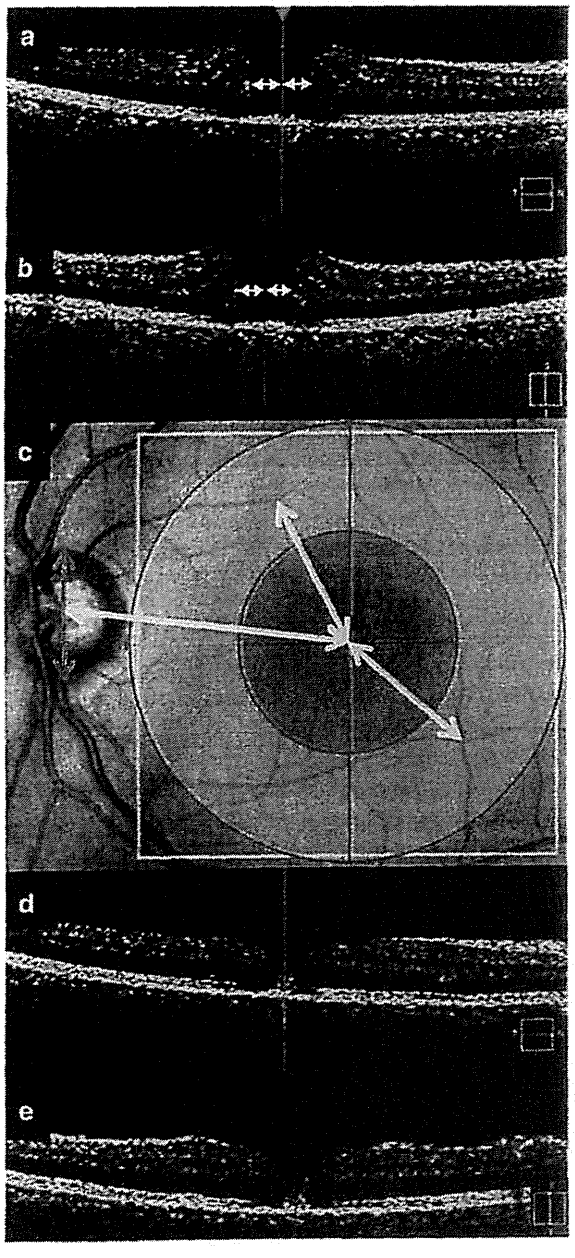

Figure 1 Diagrams of how the distances between center of MH or postoperative fovea and major landmarks are measured in the OCT images and infrared line scanning ophthalmoscope images. (a, b) Preoperative OCT images. (a) is an image obtained by a horizontal scan and (b) is a vertical scan in the raster map program of Cirrus OCT. Pink line in (a) indicates the location of the vertical scan (b). Blue line in (b) indicates the location of the horizontal scan (a). Center of MH can be easily identified by moving the location of scans (blue and pink lines) to the center of MH (white arrowheads). (c) Distance between the center of the macular hole and optic disc or bifurcation or crossing of retinal vessels were measured manually using the caliper function of the Cirrus OCT (yellow arrows). Vertical diameter of the optic disc was also measured similarly (blue arrow). The location of a bifurcation or crossing of retinal vessels were made in four areas of the macular area; inner nasal, inner temporal, outer nasal, and outer temporal area. The diameter of the ring is two and four DD (red circles). The vertical line running through fovea divided the retina into nasal and temporal halves (red vertical line). (d, e) Postoperative OCT images. (d) is an image obtained by a horizontal scan and (b) is a vertical scan in the raster map program of Cirrus OCT. Pink line in (d) indicates the location of the vertical scan (e). Blue line in (e) indicates the location of the horizontal scan (d). Center of fovea can be easily identified by moving the location of scans (blue and pink lines) to the center of fovea.